INORGANIC CHEMISTRY FRONTIERS

REVIEW

View Article Online
View Journal

Cite this: DOI: 10.1039/d6qi00068a

Detection and capture of highly toxic H_2S in porous cage-like materials: MOFs, COFs and POCs

Pablo Marín-Rosas,[a] Antonio Hernández-Monsalvo,[b] M. A. Estrella-Gutiérrez,[c] Nora S. Portillo-Veléz,[a] Jose Antonio de los Reyes,[d] Diego Solis-Ibarra,*[b] Ricardo A. Peralta*[a] and Ilich A. Ibarra*[b]

Received 12th January 2026,
Accepted 14th April 2026

DOI: 10.1039/d6qi00068a

rsc.li/frontiers-inorganic

Hydrogen sulfide (H_2S) is a corrosive and toxic gas produced naturally and mostly by industrial activity. Hence, the capture and detection of this gas is imperative, and investigations have flourished over the past decades. Adsorption by porous materials has presented a novel alternative for this problem. Materials like Metal–Organic Frameworks, Covalent–Organic Frameworks, and Porous–Organic Cages offer properties such as large surface area and tunable pore sizes that can interact effectively with H_2S. Capture and detection using these materials present new lines of investigation that could substitute other methods in the future. This review summarizes examples of these materials for the capture and detection of the toxic gas H_2S and highlights the importance of continuing these lines of study for short-term remediation.

Introduction

Hydrogen sulfide (H_2S) is a toxic compound that can be naturally found in hot springs, volcanoes, lakes, water, petroleum, and natural gas wells. Human activities can produce this gas through petroleum refining, natural gas treating, or biogas production in municipal waste and sewerage.[1] This colorless gas is corrosive and flammable, presents a distinguishable "rotten egg" odor and is toxic to humans because it rapidly enters the bloodstream, disrupting cellular oxygen absorption.[2] H_2S becomes lethal at concentrations above 100 ppm, causing permanent damage to the respiratory, cardiovascular, and nervous systems, resulting in conditions such as laryngitis, pneumonia, bronchitis, and pulmonary edema.[3] As an air pollutant, H_2S causes environmental damage due to its role in acid rain formation and its toxic properties.[4] Current methods for separating H_2S from gas streams include reactive and non-reactive absorption techniques using alkanolamines or ionic liquids, adsorption on zeolites, metal oxides, activated carbon, membrane separation, and cryogenic distillation.[5] These methods present several drawbacks, including pipe corrosion, the generation of large volumes of wastewater, low gas recovery rates, and costly reuse processes. The industrial sector needs improved adsorbents and waste management systems to achieve efficient H_2S capture, as current methods do not meet performance requirements.[6]

Porous cage-like materials present an interesting solution to this problem, and a great number of studies have focused on the use of these materials for the capture and detection of important gases such as H_2S. However, it is important to distinguish between extended structures and discrete cages. Metal–Organic Frameworks (MOFs) and Covalent–Organic Frameworks (COFs) are crystalline solids composed of infinite periodic networks, in which porosity and cavities arise from the long-term arrangement of metal nodes or organic building blocks within an extended network.[7–10] In contrast, Porous–Organic Cages (POCs) and Metal–Organic Cages (MOCs) are finite, discrete molecular entities that possess intrinsically defined internal cavities within a single molecular unit.[11–14] Despite these structural differences, both classes of materials share a functional characteristic: the presence of well-defined cavities capable of hosting guest molecules, thereby mimicking encapsulation processes. From this functional perspective, grouping extended structures and discrete cages is conceptually significant for applications such as H_2S capture and detection, where accessibility and specific bond interactions govern performance in these classes of materials. To the best of our knowledge, there are no reviews that consider all of these materials for the capture and detection of toxic H_2S.

[a]Departamento de Química, División de Ciencias Básicas e Ingeniería, Universidad Autónoma Metropolitana-Iztapalapa, 09340 Ciudad de México, Mexico. E-mail: rperalta@izt.uam.mx
[b]Laboratorio de Fisicoquímica y Reactividad de Superficies (LaFReS), Instituto de Investigaciones en Materiales, Universidad Nacional Autónoma de México, Circuito Exterior s/n, CU, Del Coyoacán, 04510 México D.F., Mexico. E-mail: argel@unam.mx,diego.solis@unam.mx
[c]Facultad de Ingeniería Química, Universidad Autónoma de Yucatán. Periférico Norte, Kilómetro 33.5, Tablaje Catastral 13615, Chuburná de Hidalgo Inn, C.P. 97203, Mérida, Yucatán, Mexico
[d]Departamento de Ingeniería de Procesos e Hidráulica, División de Ciencias Básicas e Ingeniería, Universidad Autónoma Metropolitana-Iztapalapa, 09340 Ciudad de México, Mexico

Capture and detection of hydrogen sulfide

Initially, the search for efficient and economical technologies such as catalytic oxidation[15] and Claus process[16,17] have been used for the capture of H_2S. However, adsorption is one of the most common processes for removing this toxic gas, in which molecules of a fluid (adsorbate) adhere to a solid surface (adsorbent). This phenomenon can be classified as chemisorption and physisorption. Chemisorption involves strong interactions between the adsorbate molecules and the adsorbent, resulting from the formation of chemical bonds (ionic or covalent). Chemisorption commonly requires drastic conditions to desorb the molecules from the material. On the contrary, physisorption is a reversible process where weak interactions are involved (*e.g.* van der Waals forces, dipole–dipole interactions or hydrogen bonds), the adsorbents are adhered to the surface of the material and can be removed by increasing the temperature or reducing the pressure of the system.[18,19] A desirable adsorbent material should consider important features, such as high selectivity, recyclability, chemical and thermal stability.[20]

On the other hand, the need for accurate and rapid H_2S detection has increased significantly in recent years. Exposure to H_2S at low concentrations (1–10 ppm) can produce fatigue and other discomforts; at higher levels (>500 ppm), it can be extremely dangerous and potentially lethal.[21,22] Additionally, H_2S is one of the most widely generated inorganic compounds in industry. To date, multiple strategies have been proposed for the detection of this gas, including gas chromatography, electrochemical techniques and colorimetric methods. However, due to this high gas diffusion capacity and reactivity, conventional approaches are limited in their ability to enable continuous, real-time monitoring.[23,24] Over the last decades, studies have focused on synthesizing materials with high surface area, tunable pore sizes, and stability. Hence, porous materials such as MOFs, COFs and more recently POCs have emerged as promising solutions for the capture and detection of toxic gases (*e.g.*, H_2S). Hence, one of the most important challenges in recent years is the study of the nature and strength of interactions between host molecules and different materials (Fig. 1). Each instance is conducted by a distinct mechanism, shaped by intrinsic variables related to the structural architecture and chemical composition of the adsorbent. Nevertheless, it is possible to identify key characteristics that facilitate the specific interactions between the molecules and the target material. Through the strategic selection of building blocks and architecture, researchers can precisely restrict, enhance, or modulate the interactions of these porous materials with H_2S molecules.

A primary modifiable property is the pore size. Generally, the objective is to acquire internal cavities with dimensions that do not sterically restrict the access and subsequent diffusion of molecules (for H_2S, the diameter is ≈3.6 Å).[25] Indifferent to the topology of the cavities, whether discrete

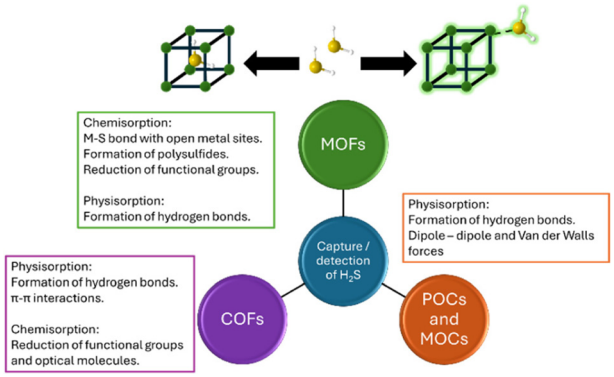

Fig. 1 Different interactions between H_2S and porous cage-like materials.

pores or interconnected crosslinked channels, steric selectivity can be achieved by size-based exclusion of larger gaseous species.[26] The nature of the intermolecular bonding represents another critical variable. For controlled capture-and-release cycles where reversibility is preponderant, weak physisorption is typically preferred. For example, electron-rich molecular systems (*e.g.*, hydroxyl groups, N-containing species, and π–π systems) are frequently used to facilitate labile associations with H_2S.[23,27–31]

Conversely, chemisorption is facilitated by the presence of free metal ion species (unsaturated metal centers or open metal sites) within coordination systems. These active centers not only foster specific chemical interactions but also serve as catalytic sites for the oxidative conversion of H_2S into elemental sulfur or polysulfides. Chemisorption-based mechanisms are particularly favorable in applications where chemical reactivity takes precedence over adsorption reversibility.[29,32–35] The incorporation of active sites may be achieved through the strategic design of the basic architecture or through post-synthetic functionalization.[23,28,36–39] Regardless of the intended application, maximizing the accessibility of these sites is crucial to ensure unrestricted gas binding. Consequently, the rigorous activation of the porous material prior to H_2S exposure is essential. This process ensures open access to the internal cavities and prevents the blockage of active sites, thereby optimizing the adsorption capacity of the material. However, the investigations into these novel materials and their interactions with toxic gases must continue to resolve this environmental issue. In the next sections, we will discuss the use of these porous cage-like materials for the effective capture and detection of H_2S and their possible applications in real systems for environmental remediation.

Metal–organic frameworks

Metal–Organic Frameworks (MOFs) represent a highly crystalline hybrid material class that shows outstanding ability to capture and store gases, including CO_2, and demonstrates exceptional potential for corrosive gas adsorption of H_2S and SO_2. The structures are formed by metal-ion or metal-cluster

secondary building units (SBUs) that combine with organic carboxylic or nitrogenous linkers, achieving stability through coordination bonds (metal–ligand interaction).[8,40] Scientists use the organic–inorganic structure of these materials to develop one-dimensional (1D), two-dimensional (2D) or three-dimensional (3D) networks through modifications of metal center geometry and ligand coordination patterns.[41] MOFs present advantages over traditional porous materials (*e.g.*, zeolites and activated carbons) owing to properties such as higher surface area or porosity, and tunable structure, this can be presented in enhanced performance in several applications. Scientists have documented more than 90 000 MOF structures while computer models predict over 500 000 additional structures that include IRMOFs, PCNs, MILs, ZIFs, UiOs, and CPLs.[40] The ability to design MOFs through synthesis enables their use in adsorption applications, catalysis, chemical detection, gas storage, and separation. MOFs also contain active sites within their porous structure, including unsaturated metal centers that enhance their ability to detect gas molecules. The performance of sensors depends on their morphology and architecture, with flexible MOFs well-suited to portable devices and rigid MOFs performing best in fixed installations requiring stable operation. MOF-based detection techniques include colorimetric,[42,43] fluorescence[44,45] and electrochemical methods.[46,47] However, the operation of MOF-based H_2S detectors and sensors faces major obstacles because metal node sulfidation, material deactivation and low conductivity result in permanent responses and structural breakdown. Scientists have only recently begun developing MOF-based H_2S sensors, as they can use structural optimization and functionalization methods to enhance operational stability.[36]

Capture of H_2S in MOFs

In general, the capture of H_2S by MOFs proceeds through physisorption and chemisorption. Physisorption involves weak interaction between the framework and the H_2S molecules, with adsorption energies ranging approximately from −40 to −10 kJ mol^{-1}. In contrast, the principal chemisorptive interactions in MOF-based systems include covalent bonding, coordination linkages between H_2S and metal centers (SH_2S–M), as well as ionic and hydrogen bonding contributions.[32] One of the first studies was presented in 2012, where Morris and collaborators demonstrated the use of Ni-CPO-27 for H_2S storage and release applications.[33] Brunauer–Emmett–Teller (BET) analysis showed a surface area of 1193 m^2 g^{-1} after activation at 150 °C. The metal sites in Ni-CPO-27 become available for H_2S binding after vacuum heating at 150 °C. The activation removes both pore water and water molecules that bind to nickel centers. The adsorption capacity of Ni-CPO-27 reaches 12 mmol g^{-1} when it interacts with H_2S at room temperature. The first part of the isotherm shows strong gas adsorption at low pressure levels. The initial stage of H_2S adsorption on Ni-CPO-27 occurs *via* chemisorption at metal sites, which are exposed to the surface of the material, according to experimental results and theoretical calculations. The binding of the H_2S molecule to the nickel sites was verified through powder X-ray diffraction (PXRD) and pair distribution function analysis (PDF). The determined Ni–S bond length ranged from 2.55 to 2.59 Å. This matches the bond lengths observed in zeolites containing the same gas, confirming specific chemisorption rather than physisorption. The differential PDF analysis proved the interaction between the gas and metal sites, and the absence of Ni–OH_2 peaks showed that metal sites were occupied by H_2S molecules instead of water.

A complementary work was presented in the use of Ni-CPO-27 (also known as Ni-MOF-74) for the adsorption of H_2S by Bordiga and collaborators.[37] The BET surface area reached 1200 m^2 g^{-1} when Ni-MOF-74 underwent activation at 200 °C under vacuum. The H_2S capture process in this material occurs through direct binding of the gas to the open metal sites. The solid changes from pale yellow to dark green when it reacts with gaseous H_2S under moderate pressure due to the strong attraction the gas has for the metal centers. The lattice contains stable Ni–S bonds, as indicated by infrared (IR) and Raman spectroscopy, that show S–H bond vibrations at lower frequencies than those of free gas molecules. The d–d electronic transitions of nickel ions undergo substantial changes according to UV-visible analysis, which demonstrates that H_2S binds directly to the metal coordination sphere. The PXRD results show that the crystal structure remains intact after prolonged H_2S exposure because the material withstands the corrosive nature of the gas. The adsorption isotherms measured by volumetric and calorimetric methods show Type I behavior, which reaches saturation at pressures lower than 1 mbar to match the usual H_2S levels present in biogas and natural gas streams. The H_2S capture capacity of Ni-MOF-74 reaches 17 wt% when all metal sites become accessible. The microcalorimetric measurements showed that the differential heat of adsorption remained constant between 56 and 58 kJ mol^{-1} until the H_2S coverage reached 0.7 mol per mole of MOF. The nickel centers in the material exhibit strong, reversible coordination bonds with the adsorbed gas molecules due to their medium-to-strong interactions. Finally, the material exhibited reversible gas adsorption at 200 °C, indicating its potential for continuous adsorption cycles.

In 2018, Ibarra and collaborators presented MOF Mg-CUK-1 as a highly promising material for capturing acid gases, particularly H_2S.[27] This metal–organic framework is constructed from Mg(II) ions coordinated to pyridine-2,4-dicarboxylic acid, forming chains of $[Mg_3(\mu_3\text{-}OH)]^{5+}$ triangles linked by hydroxyl groups. The structure crystallizes in a corrugated lattice that generates one-dimensional channels with cross-sections of 8.1–10.6 Å, large enough to allow the diffusion of small molecules such as H_2S. One of the advantages of this material is the synthesis using water as a solvent under microwave-assisted heating, which confers not only a low environmental impact during its preparation but also remarkable hydrolytic stability. The capture of H_2S on Mg-CUK-1 is explained by the moderate interaction between the gas molecules and the hydroxyl groups of the framework. Diffuse reflectance infrared Fourier-transform spectroscopy (DRIFTS) revealed that these

interactions are primarily established through hydrogen bonds, with the μ_3-OH groups acting as donors and the sulfur atoms as acceptors. Monte Carlo simulations confirmed that preferential adsorption sites are located around the hydroxyl groups and the carboxylate oxygens, with characteristic distances of 2.7–3.3 Å. This indicates that the capture does not follow an irreversible chemisorption mechanism, but rather a strong and reversible physisorption, allowing for the regeneration of the material under mild thermal activation conditions. Adsorption experiments were conducted in the gas phase at room temperature, using H_2S mixtures in nitrogen at different concentrations. As the feed concentration increased to 15%, the capacity of Mg-CUK-1 increased proportionally, reaching approximately 3.1 mmol g^{-1}. Furthermore, the capacity remained constant at approximately 3.2 ± 0.2 mmol g^{-1} after five adsorption–desorption cycles, demonstrating high reversibility. The stability of the framework was confirmed by PXRD, and the material retained crystallinity, reinforcing its robustness under realistic operating conditions. The adsorption enthalpy calculation at low loading rates yielded a value of −23.3 kJ mol^{-1}, consistent with a moderate interaction, sufficient to ensure selectivity without compromising regeneration.

In 2021, Milner *et al.* studied biocompatible MOFs for H_2S capture and release management.[48] The research employed three Zr-based MOFs (termed Zr-fum, Zr-mes and Zr-ita) using linkers from natural acids; fumaric, mesaconic and itaconic respectively (Fig. 2a). The BET surface area measurements showed that Zr-fum reached 800 m^2 g^{-1} while Zr-ita reached 235 m^2 g^{-1} and Zr-mes showed intermediate values. The gas-phase H_2S capture studies were performed through adsorption isotherm measurements at temperatures from 25 °C to 55 °C (Fig. 2b). The research showed Zr-fum had the highest adsorption capacity at 4.0 mmol g^{-1} (approximately 11 wt%) followed by Zr-mes at 3.3 mmol g^{-1} (approximately 10 wt%) and Zr-ita at 1.3 mmol g^{-1} (approximately 4 wt%). The Density Functional Theory (DFT) simulations demonstrated that H_2S molecules bind to the metal clusters through O–H···S interactions with OH^- groups and S–H···S bonds between confined H_2S molecules which explains the observed stability and reversibility. Additionally, the stability of the material was tested, as the porosity of the MOF was retained throughout multiple adsorption–desorption cycles. Finally, the system releases H_2S when it comes into contact with biological aqueous solutions (*e.g.*, Phosphate–Buffered Saline (PBS) and cell culture medium). The binding sites in the cavities become available to water molecules, which then release the trapped gas into biological environments. The fluorescence tests showed that the system produced H_2S at rates equivalent to biological tissue while remaining non-toxic to HeLa cells.

In 2019, MOF MIL-53(Al)-TDC was used for both H_2S resistance and outstanding gas capture ability.[49] The material showed an adsorption capacity of 18.1–18.6 mmol g^{-1} at 30 °C and 1 bar, which resulted in 618 mg of H_2S per gram of material. The results showed that H_2S spread uniformly through pores according to both gravimetric analysis and Monte Carlo simulation methods. IR spectroscopy experiments verified that the gas capture process depends on weak and reversible interactions. The channels of the material allowed H_2S molecules to form dimers through hydrogen bonding as the gas concentration rose. The material stored H_2S at high levels due to weak intermolecular bonds, enabling both high storage capacity and simple low-temperature regeneration. The MOF crystal structure remained stable during multiple adsorption–desorption cycles, as indicated by PXRD and Scanning Electron Microscopy (SEM) results. The MOF structure of

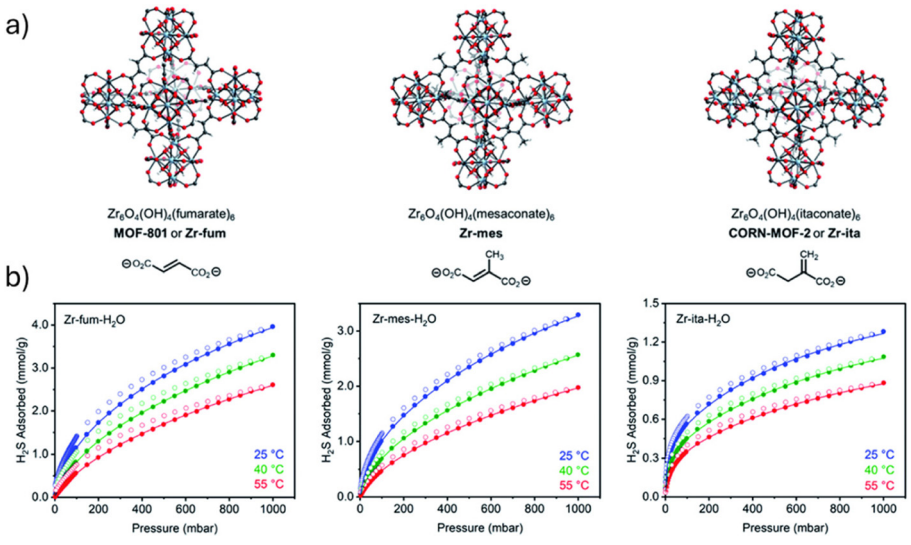

Fig. 2 (a) Density functional theory-calculated ideal structures of the metal–organic frameworks prepared from fumaric, mesaconic, and itaconic acid. Color code: Zr = blue, C = gray, O = red and H = white. (b) H_2S adsorption (closed circles) and desorption (open circles) isotherms at 25 °C (blue), 40 °C (green), and 55 °C (red) of activated Zr-fum-H_2O, Zr-mes-H_2O, and Zr-ita-H_2O. Adapted from ref. 48 with permission from Royal Society of Chemistry, copyright 2021.

MIL-53(Al)-TDC enables full H_2S desorption through material reactivation at 200 °C under dry nitrogen or at 65 °C according to high-resolution thermogravimetric analysis (TGA). The adsorption enthalpy of −23.2 kJ mol^{-1} shows that the gas interactions are strong enough for retention but weak enough for efficient regeneration. The material maintained a stable adsorption capacity of 18.5 ± 0.7 mmol g^{-1} over five consecutive cycles, retaining its crystal structure demonstrating stability upon H_2S exposure. In 2022, Humphrey and collaborators reported the synthesis of MOF Mn-CUK-1 for the efficient capture of H_2O, SO_2, and H_2S.[28] The material was prepared with Mn(II) as the metal node and pyridine-2,4-dicarboxylic as the linker (Fig. 3a). One of the properties of the material is structural flexibility, which allows the unit cell volume and channel shape to change upon interaction with host molecules. Adsorption experiments were performed in the gas phase at 1 bar and room temperature. After the activation at 200 °C, Mn-CUK-1 reached an adsorption capacity of up to 16.5 mmol g^{-1} for H_2S and an average uptake capacity of 13.65 mmol g^{-1} after 5 cycles (Fig. 3b). The stability of the framework was confirmed by PXRD as the pattern matched the fresh sample, showing chemical resistance to the corrosive gas H_2S. The combination of the defined channels, hydroxyl groups, and a flexible framework enables Mn-CUK-1 to capture H_2S.

In 2021, Ibarra and collaborators demonstrated that the MOFs SU-101 and MFM-300 (In, Sc) can capture gaseous H_2S and transform it into polysulfides *via* chemical reactions within their pores under mild conditions.[34] For the adsorption using the MFM-300 materials, the experiments were performed at 25 °C under 1 bar pressure. MFM-300(Sc) captured 16.5 mmol of sulfur per gram of material during the first stage; the material maintained the crystalline structure after multiple adsorption cycles, but lost part of its pore volume due to sulfur compounds that remained inside the material. During subsequent adsorption cycles, MFM-300(Sc) presented adsorption of 10.2 mmol g^{-1}. The combination of DRIFTS, Raman spectroscopy, and elemental analysis showed that the trapped species included various polysulfide chains with different lengths (S_2^{2-}, S_4^{2-}, S_6^{2-}), which proved that the process involved chemical transformations inside the pores. The first adsorption capacity of MFM-300(In) reached 9.1 mmol g^{-1}; however, the material showed complete pore blockage from sulfur species retention. The material lost all its capacity after the first cycle due to high-order polysulfides that blocked all available channels. Raman spectroscopy and electrochemical tests confirmed the presence of extended polysulfide species, which caused the material to lose all its available pore space. Additionally, MOF SU-101 was tested for the capture of H_2S, this material contains bismuth (Bi^{3+}) ions, that form a biocompatible structure with elagate ligands. This material presents open metal sites (OMS), which operate as primary binding sites that enable direct H_2S molecule attachment. SU-101 achieved a breakthrough H_2S adsorption capacity of 15.95 mmol g^{-1} at room temperature and atmospheric pressure despite its low BET surface area (412 m^2 g^{-1}). The material lost most of its adsorption ability after the first cycle, but maintained its crystalline structure while the surface area decreased to 15 m^2 g^{-1}. The Raman spectroscopy results showed that sulfur molecules formed low-order polysulfides (S_4^{2-}) through bonding with open Bi^{3+} centers. The proposed mechanism for both materials is similar (Fig. 4); the process starts with the adsorption of H_2S gas molecules and binding to the metal center. The –SH species then form a bond, resulting in the production of H_2 and S–S formation, which initiates polysulfide chain development. A complementary work was presented in 2024, as the H_2S-saturated SU-101 material was used as a lithium–sulfur battery cathode.[50] The study proved that the polysulfides present in the framework can serve as electroactive materials without requiring artificial sulfur addition to the electrode. The system converts dangerous environmental pollutants into useful energy storage materials through its complete recycling process. The electrochemical tests of SU-101 electrodes with H_2S showed 85 mAh g^{-1} initial capacity and maintained 54% capacity retention through 1000 cycles at 99.8% coulombic efficiency. The battery showed excellent stability due to the Bi^{3+} centers strongly bonding with polysulfides, thereby preventing leakage and minimizing the shuttle effect that causes performance degradation in these batteries. These studies presented an important breakthrough in the use of MOFs for the capture of toxic H_2S and for promoting waste valorization in applications such as energy storage.

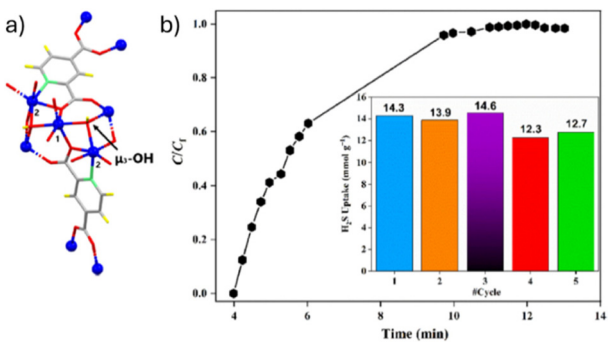

Fig. 3 (a) Expanded asymmetric unit of microwave synthesized Mn-CUK-1. (B) H_2S breakthrough curves at 298 K and 1 bar with adsorption capacity (in inset). Adapted from ref. 28 with permission from American Chemical Society, copyright 2022.

Detection of H_2S in MOFs

Alternatively, MOFs have emerged as outstanding candidates for H_2S detection due to their modular architecture and molecular sieving effect, which facilitate analyte preconcentration and enhance selectivity through specific matrix interactions. To broaden their practical applicability, it is essential to continue modifying and functionalizing MOFs to optimize their performance as H_2S detection platforms.[23,24] In 2015, Yi Lv *et al.* explored the use of MOFs as sensitive materials for H_2S detection by cataluminescence (CTL).[35] Specifically, the group evaluated four MOFs: MIL-100(Fe), MIL-101(Cr),

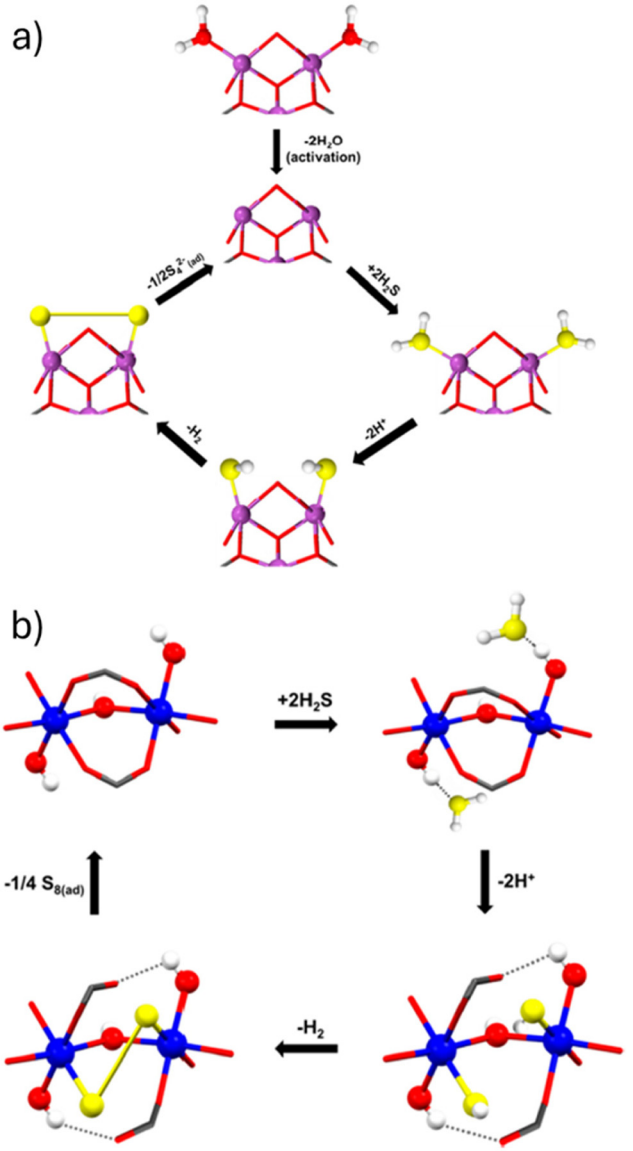

Fig. 4 Schematic representation of the proposed catalytic mechanism for the transformation of H_2S to polysulfides in (a) SU-101 and (b) MFM-300 (Sc). Color code: Bi = purple, Sc = blue, O = red, S = yellow and H = white. Adapted from ref. 34 with permission from American Chemical Society, copyright 2021.

$Zn_3(BTC)_2{\cdot}12H_2O$, and ZIF-8, aiming to identify structures that combine stability, sensitivity, and selectivity for gaseous H_2S. Both MIL materials showed high porosity, but adsorption tests revealed low stability: MIL-100(Fe) showed a strong CTL signal; however, the material degraded upon contact with H_2S; MIL-101(Cr) exhibited very weak signals along with structural destruction. This ruled out their practical applicability. In contrast, the zinc materials $Zn_3(BTC)_2{\cdot}12H_2O$ and ZIF-8 stood out as more promising devices. The detection mechanism relies on the catalytic oxidation of H_2S in the presence of atmospheric oxygen at the unsaturated metal sites of the MOFs, generating excited species that emit light (CTL). The experiments demonstrated that both $Zn_3(BTC)_2{\cdot}12H_2O$ and ZIF-8 responded linearly to low H_2S concentrations (15.39 ppm), with detection limits of 4.4 ppm and 3.0 ppm, respectively. Furthermore, both materials exhibited structural stability after multiple cycles and marked selectivity towards interfering compounds such as alcohols, acetone, and formaldehyde. Under these conditions, the recorded CTL signal was sufficiently intense and reproducible to propose its implementation in environmental sensors. In 2016, Eddaoudi *et al.* reported the development of a MOF using fumaric acid as a linker and yttrium as a metal center, and synthesized *in situ* on pre-functionalized capacitive interdigitated electrodes (IDEs) for the detection of H_2S.[51] Experiments conducted in a gas chamber at room temperature showed that the material is capable of detecting H_2S across a wide concentration range (100–1000 ppb), with a detection limit of 5.4 ppb. Selectivity tests confirmed that the signal for H_2S was up to six times stronger than that obtained for the most critical interfering gases, such as CH_4, NO_2, H_2 and toluene. The stability was verified over three months of continuous use with no significant loss of sensitivity or activity. The detection principle is based on the change in the film's electrical permittivity when H_2S gas molecules adsorb onto the MOF pores. The selectivity of the material, combined with structural robustness, enables a sensitive and stable detection process, without significant degradation due to the formation of metal sulfides.

In 2015, Qian and collaborators reported the design and application of a turn-on fluorescent material for the detection of H_2S based on the post synthetic modification of the IRMOF-3.[23] This MOF is characterized by the presence of free uncoordinated amino groups ($-NH_2$); taking advantage of this characteristic, the groups were transformed into azide groups ($-N_3$) through a diazotization reaction (Fig. 5). The resulting product, designated IRMOF-3($-N_3$), was tested for the selective detection of H_2S; the system responded immediately to the presence of this gas, showing a pronounced increase in emission intensity centered at 430 nm upon excitation at 395 nm. The response stabilized in less than two minutes, representing a shorter detection time than most conventional azide sensors, which typically require between 20 minutes and 2 hours. Regarding selectivity, the material showed remarkable resistance to interference from biologically relevant species (*e.g.* glutathione, cysteine, homocysteine) and common anions (NO^{3-}, PO_4^{3-}, Cl^-), causing minimal changes in the intensity

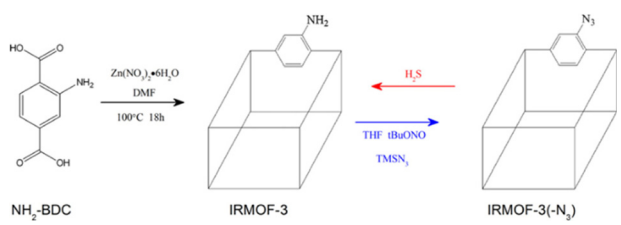

Fig. 5 Schematic illustration of design of MOF-based selective turn-on probe for H_2S. Adapted from ref. 23 with permission from Elsevier, copyright 2015.

of the signal. The detection principle is based on a selective reduction process mediated by H_2S. In the presence of this gas, the azide group is reduced to an amino group, which generates a drastic change in the electronic properties of the material. While IRMOF-3($-N_3$) exhibits weak fluorescent emission due to the strongly electron-withdrawing nature of the $-N_3$ group, reduction to $-NH_2$ restores internal charge transfer (ICT) flow, resulting in a marked increase in fluorescence intensity. This change forms the basis of the turn-on mechanism, allowing the material to act as a fast, sensitive, and selective optical device. Later, the same group presented a study on the development of a highly sensitive and selective fluorescent detector based on a vinyl-functionalized zirconium MOF, called UiO-66-CH=CH_2.[52] The MOF was synthesized in water, generating nanoparticles 20–30 nm in size and a specific surface area of 868.8 $m^2\ g^{-1}$. The PXRD analysis demonstrated the stability of the material in aqueous media after three days without loss of crystallinity. Detection was performed under physiological conditions (HEPES buffer), using NaHS as a source of H_2S. In its original state, the material exhibits intense blue emission. Upon exposure to H_2S, a drastic quenching of the fluorescence was observed. The detection principle is based on the breaking of the vinyl double bond in the framework by the reducing action of H_2S, which causes the destabilization of the aromatic conjugate system, decreasing the emission intensity (turn-off mechanism). FTIR analysis confirmed that, upon interaction with H_2S, the C=C stretching band at 1652 cm^{-1} disappears, confirming the cleavage of the vinyl group. The PXRD pattern of the sample remained unaltered, indicating that the framework retains its overall structure despite the local reaction. Additionally, the detection performance of UiO-66-CH=CH_2 toward H_2S was tested, showing negligible fluorescent signal against other species, demonstrating the selectivity of the material; making UiO-66-CH=CH_2 an ideal candidate for detection applications.

In 2020, Wang *et al.* reported a copper metal–organic framework, termed Cu-HIA, constructed from Cu(II) ions, 5-hydroxyisophthalic acid, and 4,4′-bipyridine.[29] The material was used for the fluorescence detection of H_2S under physiological media (Na_2S was used as H_2S source). After exposure to the H_2S, the disappearance of a signal around 350 nm was observed (associated with metal–ligand charge transfer), while the intensity of a signal at 410 nm increased. This is attributed to the organic ligand. Furthermore, the material exhibits high selectivity against reducing biological molecules and other anions (*e.g.*, NaCl, NaBr, NaI, $NaNO_2$ and $NaNO_3$). However, a distinctive feature of Cu-HIA is that interaction with H_2S causes the progressive degradation of the MOF, evidenced by a color change from blue to black. This was corroborated by FTIR and PXRD analyses, which showed patterns consistent with the appearance of CuS. This transformation explains the disappearance of the metal–ligand emission and the recovery of the organic ligand's luminescence. In 2021, Mahmoud *et al.*, developed a flexible, low-power and highly sensitive material for H_2S detection under ambient conditions.[53] The group incorporated MOF-5 microparticles into a chitosan (CS) polymer matrix modified with a glycerol ionic liquid (IL). The final device, termed MOF-5/CS/IL, was integrated into a copper and stainless-steel electrode system and its response was evaluated under exposure to different concentrations of gaseous H_2S. The detection is based on the acid–base interaction between the gas and the amino groups of chitosan, as well as the coordinated oxygen atoms of MOF-5. These interactions facilitate proton transport across the membrane, resulting in a change in the measured current. MOF-5, thanks to its high density of oxo sites and porous structure, provides additional channels for transport and adsorption, improving overall sensitivity (Fig. 6). The stability of MOF-5/CS/IL was confirmed through repeated cycles over 21 days, maintaining a detection efficiency of 96–98%. Selectivity was demonstrated against other common gases such as H_2, CO and C_2H_4, with considerably lower responses. This work demonstrated the use of MOFs in flexible membranes for H_2S detection and their future applications in monitoring air pollution.

More recently, in 2025, Ibarra and collaborators introduced a novel strategy for H_2S detection using SU-101.[54] Previously, the group demonstrated the use of this material for the capture of H_2S and its subsequent transformation into polysulfide species within the pores of the material. Consequently, the fluorescence detection of H_2S using SU-101 was performed. The formation of the polysulfide species increases the rigidity of the framework and partially restricts the ligand-to-metal charge-transfer (LMCT) pathway (Fig. 7a). As a result, non-radiative deactivation channels are suppressed while radiative emission is enhanced, yielding a pronounced fluorescence "turn-on" response in the material (Fig. 7b). Spectroscopic analyses using Raman, X-ray Photoelectron Spectroscopy (XPS), and UV-Vis techniques confirmed the formation of these polysulfide species and their influence on the optical properties of SU-101. Complementary DFT calculations indicated that the interaction of polysulfides within the pores is energetically favorable, and that the chain length of the sulfur species plays

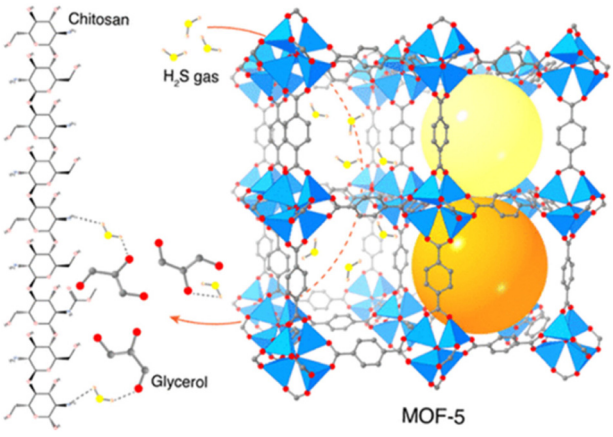

Fig. 6 Illustration of the suggested H_2S gas-sensing mechanism. Color code: Zn = aqua, S = yellow, N = blue, O = red, C = gray and H = pink. H atoms on MOF-5 are omitted for clarity. Adapted from ref. 53 with permission from American Chemical Society, copyright 2021.

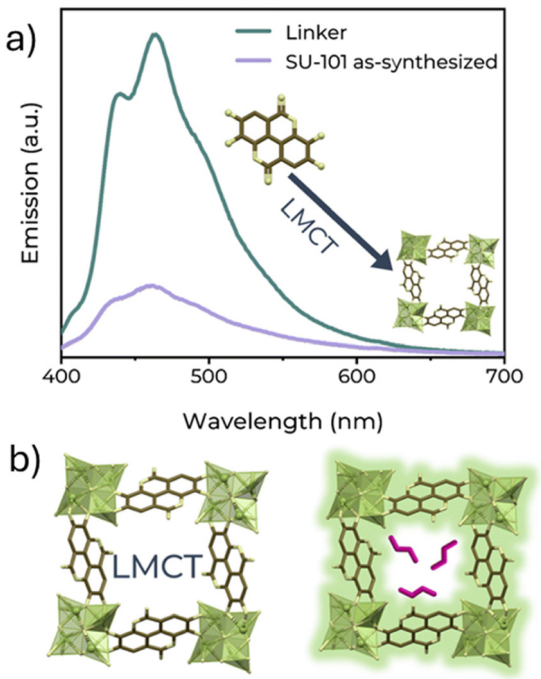

Fig. 7 (a) Solid-state emission spectra of the ellagic acid linker and as-synthesized SU-101. (b) Schematic of the changes of pristine and H_2S-saturated SU-101 material. Adapted from ref. 54 with permission from Royal Society of Chemistry, copyright 2025.

a decisive role in the resulting optical response. The MOF achieved a detection limit of approximately 22 ppm for H_2S, highlighting its potential as a promising candidate for environmental monitoring and industrial safety applications. Additionally, SU-101 exhibited a highly selective response, as other molecules such as CO_2 and H_2O produced no noticeable changes in fluorescence. Thus, SU-101 proved to be an excellent candidate for detection applications. Over the last decades, MOFs have been one of the most studied materials for several applications, including the capture and detection of toxic gases (*e.g.* H_2S). However, stability of the framework was an issue at the beginning of the studies due to the acidity of this gas; the use of adequate metals and topologies made a difference in the performance of the materials. MOFs can also serve as a solution, since the formation of species such as polysulfides within the framework can be used to form cathodes for batteries and to valorize waste. Additionally, the rapid detection of H_2S using these materials has been demonstrated selectivity and recycling that are important factors that other materials do not offer, making them excellent candidates for further studies and improvements. These results show that MOFs are an interesting alternative for these applications. However, future studies are needed to take the next step; the scalability of these materials and their integration into new devices could present a solution for industrial applications. Despite these challenges, MOFs present as promising solutions for the capture and detection of H_2S in the near future.

Covalent–organic frameworks

Covalent–Organic Frameworks (COFs) are a class of porous materials constructed from organic monomers *via* covalent bonds and constituted of light elements (*e.g.* C, N, O, B and S). COFs offer interesting properties, such as high porosity and large surface area. Since they are metal-free materials, other advantages over conventional porous materials are low toxicity, low density, and high stability arising from the robust covalent bonds in their structure.[55–58] In 2005, Yaghi and collaborators presented the synthesis of the first COFs under solvothermal conditions, COF-1 and COF-5 presented high surface areas (711 and 1590 $m^2\ g^{-1}$, respectively) and high thermal stability (up to 500–600 °C).[9] Since then, COFs have gained attention for their diverse linkages and topologies across applications such as catalysis, energy storage, water treatment, drug or enzyme delivery, gas storage and separation.[59–62] In this section, we discuss the importance of COFs and their use as a potential solution to environmental pollution in the capture and detection of the toxic gas H_2S.

Capture of H_2S in COFs

COFs have demonstrated efficiency as adsorption agents in the removal of harmful gases. The large surface area and porosity in their structure present an opportunity for the capture of various gases (CO_2, NO_X, SO_2, NH_3 and H_2S).[55,63,64] For example, Jiang *et al.* presented a functionalized COF for the capture of CO_2.[65] The material, termed [HO_2C]100%-H_2P–COF, showed high adsorption (180 mg g^{-1}) and selectivity toward CO_2. Under high vacuum at 80 °C, the material could be regenerated without a decline in activity after ten cycles. In 2017, Park *et al.* synthesized an imide-functionalized COF (termed PI-COF) *via* a microwave-assisted reaction for effective SO_2 adsorption.[66] The material exhibited a high surface area, resulting in an outstanding SO_2 sorption capacity of 6.3 mmol g^{-1} (41 wt%). PI-COF could be regenerated through N_2 purging and demonstrated high stability after five adsorption–desorption cycles. These results showed the importance of COFs in the capture and separation of different gases, as well as the chemical stability and recyclability of these materials for adsorption cycles. Herein, we describe the use of COFs in the capture of toxic H_2S as a possible environmental solution.

In 2021, Zheng and collaborators presented the self-polymerization of 1,4-dicyanobenzene for the elimination of H_2S.[67] The covalent triazine framework (CTF) was synthesized at different temperatures (400, 500, 600, and 400–600 °C). The PXRD pattern showed two broad peaks that indicate an amorphous carbon network. Sample CTF-1-400–600 presented a large BET surface area (3909 $m^2\ g^{-1}$), while pore analysis suggested the presence of micro–mesopores in the material. Additional XPS experiments showed tunable edge amine and graphitic nitrogen sites, which can be adjusted by the calcination temperature during synthesis. The material was tested for its ability to selectively capture acid gases, such as H_2S and CO_2. CTF-1-400–600 sample exhibited extremely high H_2S adsorption capacities (12.8 mmol g^{-1} at 0 °C and 1.0 bar).

Additionally, the material was reused in five adsorption cycles, presenting the same activity as the synthesized sample. Ideal adsorption solution theory (IAST) analysis demonstrated enhanced selectivity of the CTF material with H_2S over other gases (CO_2, CH_4 and N_2), meaning that the H_2S can be easily adsorbed from mixed gases. To avoid secondary pollution, the CTF-1-400–600 material was tested as a catalyst for the selective oxidation of H_2S to elemental sulfur. A conversion close to 100% (99.9%) was achieved at 180 °C, which was attributed to the large surface area and enhanced nitrogen content in the sample. Catalytic performance was maintained in 100% conversion for 40 h of reaction. Also, the CTF-1-400–600 sample did not present sulfur deposition on the surface; this could be due to the micro–mesoporosity in the material. A reaction pathway was proposed, where H_2S undergoes a hydrogen transfer reaction in the double layer of the material. This proposal can eliminate the competitive oxidation of other molecules, such as CO, that could affect the oxidation of H_2S (Fig. 8). Overall, the material presented excellent adsorption and catalytic activity in the presence of H_2S compared to other commercial desulfurization catalysts.

Yang and collaborators presented the synthesis of a sandwich-like core–shell structure for the photocatalytic oxidation of H_2S to elemental sulfur.[68] COF was synthesized using 1,3,5-tris(4-aminophenyl) benzene (TAPB) and 2,5-Dimethoxybenzene-1,4 formaldehyde (DMTP) (Fig. 9a). Two materials were synthesized; sample SiO_2@COF@α-Fe_2O_3 was prepared using SiO_2 as an internal layer, TAPB-DMTP-COF as a middle layer, and metal oxide (α-Fe_2O_3) as an external layer. Sample termed SiO_2@α-Fe_2O_3@COF used SiO_2 as an internal layer, α-Fe_2O_3 as a middle layer and TAPB-DMTP-COF as an external layer (Fig. 9b). Characterization of the synthesized composites (PDRX, FTIR, TEM) confirmed the core–shell structure, the photocatalytic activity of the samples was studied under LED light (420 nm) irradiation for the oxidation of gas-phase H_2S. The SiO_2@COF@α-Fe_2O_3 sample presented a removal efficiency of 95.4%. However, the activity underwent a decrease after 2 h of reaction. This could be due to the interaction of the α-Fe_2O_3 external layer and the elemental sulfur,

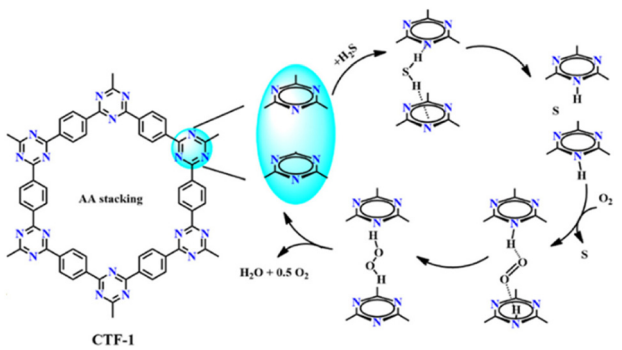

Fig. 8 Proposed mechanism of H_2S dissociation to S with the help of O_2 in double-layer AA stacking of CTF-1-*x*. Adapted from ref. 67 with permission from American Chemical Society, copyright 2021.

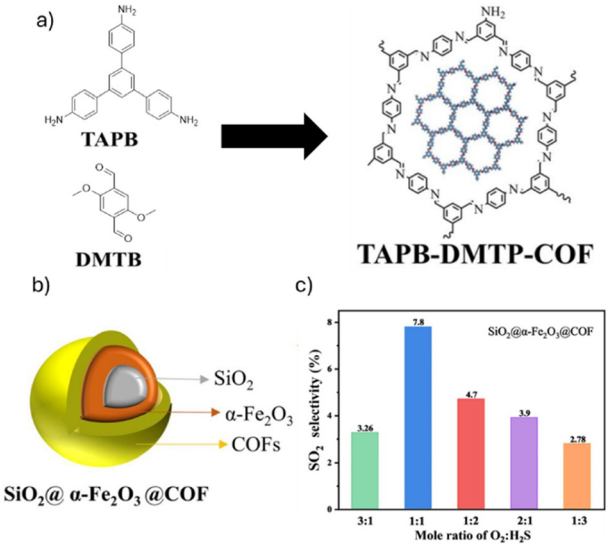

Fig. 9 (a) Synthesis of TAPB-DMTP-COF. (b) Design and synthesis process of sandwich core–shell composite structure SiO_2@α-Fe_2O_3@COF. (c) Photocatalytic activity of SiO_2@α-Fe_2O_3@COF with different oxygen/hydrogen sulfide ratios. Adapted from ref. 68 with permission from Elsevier, copyright 2023.

causing the deactivation of the material. On the other hand, SiO_2@α-Fe_2O_3@COF exhibited a removal efficiency of 95.2% for 9 h of reaction without loss of activity under different oxygen/hydrogen sulfide ratios (Fig. 9c). Additionally, the material showed the same activity in five consecutive reaction cycles, maintaining morphological and internal structural features, demonstrating stability in the photocatalytic reaction. Electron spin resonance (ESR) experiments demonstrated that electrons (e^-) and superoxide radicals ($^{\bullet}O^-_2$) are the main species involved in the effective separation of light-induced electron–hole pairs. This result, combined with the positions of the conduction band (CB) and valence band (VB), indicates the presence of S-type heterojunctions, which lead to photocatalytic activity, yielding hydrogen peroxide and elemental sulfur as final products.

In 2015, Cao *et al.* used molecular simulation to investigate the capture of sulfur gases using COFs.[69] Several 2D (COF-5, COF-6, COF-8, COF-10) and 3D (COF-102, PAF-302) COFs were selected to capture H_2S using Grand Canonical Monte Carlo (GCMC) simulations. Results indicate that the maximum excess of H_2S follows the order of PAF-302 > COF-102 > COF-10 > COF-5 > COF-8 > COF-6, which is correlated with the pore volume of the materials. PAF-302 presented the highest H_2S capture, 51.94 mmol g^{-1}, due to the large BET surface area (5600 m^2 g^{-1}), while COF-6 presented the lowest H_2S uptake of 7.927 mmol g^{-1}, due to the low surface area presented (750 m^2 g^{-1}). Selectivity experiments were performed with different gas mixtures (H_2S–N_2, H_2S–CO_2 and H_2S–CH_4), indicating that 2D materials presented higher selectivity to sulfur gases than the 3D materials. COF-6 presented the highest selectivity to H_2S in all three gas mixtures; this result is attributed to the smaller

pore size in the framework. The confinement effect is presented in the COF, which becomes beneficial for gas selectivity. This work illustrated the importance of pore size and surface area for the storage and separation of different gases in COFs and the possible applications of these materials in the capture and detection of toxic gases like H_2S.

Another computational approach was presented by Keskin and collaborators, where known COFs (from two databases) and computer-generated hypothetical COF (hypoCOF) were tested for the selective capture and separation of H_2S and CO_2.[70] First, 580 known COFs were evaluated by performing GCMC simulations in a six-component gas mixture ($CH_4/C_2H_6/CO_2/C_3H_8/H_2S/H_2O$), COF-320 and PI-COF-2 presented high-pressure swing adsorption (PSA) and vacuum-swing adsorption (VSA) values. However, COF NPN-3 showed the best performance, favoring the adsorption of H_2S and CO_2 over other gases. This could be attributed to the narrow pores and the interaction of these gases with the linker in the framework. The DFT analysis revealed that H_2S binds *via* π–π interactions and a hydrogen bond between the sulfur atom and the linker in the NPN-3 COF, demonstrating selectivity for this molecule. Additionally, hypoCOFs were studied, and the results showed that structural properties (*i.e.*, pore size, porosity) could be important factors for gas separation. However, the heat of adsorption played an important role in determining the best hypoCOFs, underscoring the importance of computational studies in the creation of new COF materials for these applications. Most of the studies for the capture of H_2S have focused on MOFs over the last years; however, there is an increase of interest in COFs as an alternative. Computational studies are required for the design and synthesis of new structures for this application; functionalization of different functional groups or guest molecules can be important for selective H_2S capture. The use of COFs in the removal of this toxic gas could present an interesting field of study over the next years.

Detection of H_2S in COFs

An interesting feature of COFs is chemical detection due to the tunability of the properties (addition of acid or basic sites, redox centers), such as robust structures, large surface and porosity, making them excellent candidates for detection platforms. Notably, these materials have been used for the detection of several gases due to their strong covalent linkage, which presents an advantage under harsh conditions.[71,72] In 2024, Zhao and coworkers presented the use of a COF for the detection of SO_2.[73] The sample, termed SonoCOF-9, showed SO_2 adsorption of 0.91 mmol g^{-1} at 0.1 bar, demonstrating good reversibility in 50 adsorption–desorption cycles. Interestingly, SonoCOF-9 presented a "turn-off" response when the sample was exposed to the SO_2. Additionally, the fluorescence of the material was not affected when exposed to air and CO_2, demonstrating selectivity as a detector of SO_2. Hence, COFs present an interesting option for the selective detection of H_2S.

The synthesis of a novel 2D COF was presented by Mirica and coworkers in 2019, the material was obtained by the condensation of NiOAPc (octaamino-derived nickelphthalocyanine) and TOPyr (pyrenetetraone) presenting a fully aromatic conjugated framework structure with square apertures.[38] The characterization of the sample (COF-DC-8) revealed the desired structure and properties of the material, with additional bulk conductivity reaching 2.51×10^{-3} S m^{-1}, significantly higher than that of similar materials, indicating the potential for use in the fabrication of electronic devices. The chemiresistivity of COF-DC-8 was tested with a series of reducing and oxidizing gases (H_2S, NH_3, NO and NO_2), the limit of detection for H_2S obtained was 204 ppb after 1.5 min of exposure. Additionally, COF-DC-8 presented increased resistance towards reducing gases. The reactivation of the COF was tested, immersing it in deionized water for 1 h, which presented excellent results as the response of the material was restored. However, after thermal activation, the response of the COF-DC-8 samples was only partially restored, suggesting that the molecules (H_2S) are bound to the material and can be released in aqueous conditions. This information is useful, so the devices can be used several times for detection applications.

In 2021, the use of a porphyrin-based nanoscale COF was presented for the selective detection of H_2S in water.[74] The material (termed CuCOF) was synthesized with 2,5-dihydroxyterephthalaldehyde and tetra(pamino-phenyl)porphyrin to obtain the desired COF. Since the addition of paramagnetic metals to porphyrins leads to the loss of the fluorescent properties,[75] $Cu(NO_3)_2$ was added to coordinate with the nitrogen atoms present in the material to form the CuCOF. The addition of NaHS (as source of H_2S) led to the release of the Cu^{2+} ions and the recovery of the fluorescent properties of the porphyrin, creating a "turn on" effect in the material (Fig. 10a). The CuCOF was tested with other thiols and anionic species, showing negligible fluorescence and demonstrating excellent selectivity towards H_2S (Fig. 10b and c). The material was tested on real water samples, demonstrating correct detec-

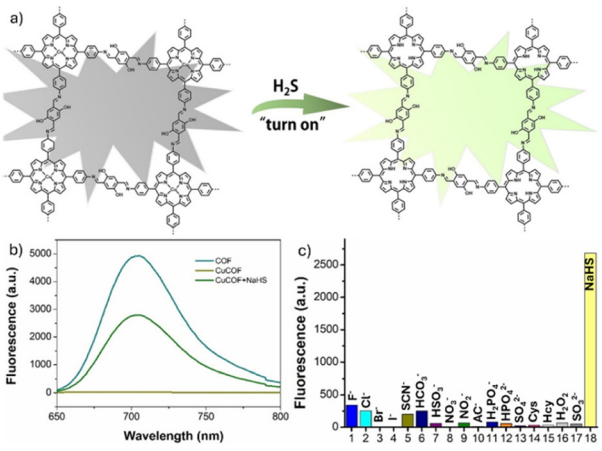

Fig. 10 (a) Scheme for fluorescent variation of CuCOF upon reactive metal centers as the binding site of H_2S. (b) Analysis of CuCOF nanoprobe towards to detect H_2S. (c) Fluorescence analysis of CuCOF nanoprobe reacted with different kinds of reactive species. Adapted from ref. 74 with permission from John Wiley and Sons, copyright 2021.

tion of H_2S, underscoring the importance of studying these materials for practical applications.

In 2018, Zhang and coworkers showed the use of a COF for the detection of H_2S in a mouse model of cirrhosis.[76] The selected COF (termed TpASH) is prepared *via* Schiff-base condensation (Tp 1,3,5-triformylphloroglucinol and ASH 4-aminosalicylhydrazide) and presents chemical stability due to irreversible enol–keto tautomerism. The COF was modified with glycol and served as a molecular anchor for NPHS (4-amino-1,8-naphthalimide derivative) (Fig. 11a). The new COF nanoprobe (termed TpASH-NPHS) was used to detect H_2S. Detection experiments were performed in a phosphate buffered solution and the addition of NaHS as H_2S source. The reduction of the N_3 group generated a significant increase in the material's fluorescence. Additionally, the COF nanoprobe demonstrated selectivity for H_2S in the presence of reactive species like common anions and bio-thiols, under normal and deficient oxygen conditions, TpASH-NPHS also presented photostability and limited cytotoxicity. Since H_2S is produced during chronic liver injury or cirrhosis, detecting this molecule could be important in the early stages of this disease. Hence, TpASH-NPHS was used to detect H_2S in the bioimaging of a mouse liver with early-stage cirrhosis. The experiment showed an increase in fluorescence, indicating disease progression related to the level of endogenous H_2S in the samples (Fig. 11b). This work presented an alternative use for COFs in the detection of important molecules for bioimaging and medicine.

In 2021, Dong *et al.* presented the synthesis of a Cu^{2+}-porphyrin-derived COF, termed Cu-DhaTph.[77] The removal of Cu^{2+} ions by adding NaHS, used to simulate endogenous H_2S under physiological conditions, enhanced the fluorescence of the material ("turn on" effect) while showing negligible fluorescence toward other ions, demonstrating excellent detection properties. Photodynamic experiments using 1,3-diphenylisobenzofuran (DPBF) were performed. Cu-DhaTph presented a quick response and an efficient $^1O_2$ generation ability. Additional UV-vis-NIR absorption spectra showed the formation of CuS *via* an *in situ* sulfidation reaction. These results presented an opportunity to use the material in a PDT/PTT (PDT = photodynamic therapy, PTT = photothermal therapy) combination treatment for colon tumor sites. Cu-DhaTph could react with endogenous H_2S to generate CuS, DhaTph can act as a photothermal agent in PTT and a photosensitizer in PDT, respectively. This study provided important advances in the use of COFs in combination therapy for colon tumor sites and H_2S detection. Finally, Wang *et al.* presented the incorporation of a fluorescent indicator, PB (sodium 1-pyrenebutyrate), into the framework of COF EB-TFP for the detection of gaseous H_2S.[78] The composite material (EB-TFP@PB) was tested for H_2S detection using an indicator displacement assay (IDA) strategy. The material exhibited enhanced fluorescence upon the addition of this gas. The EB-TFP@PB sample presented excellent selectivity as negligible fluorescence was observed in the presence of other possible interfering compounds. A reaction pathway was proposed, where the H_2S presents high affinity to EB-TPF, replacing the PB molecule from the framework, resulting in the fluorescence of the free PB molecule (Fig. 12). The presented work demonstrated that COFs can serve as supports for other molecules and as potential H_2S detectors. Although COFs were discovered in 2005, their use for the capture and detection of H_2S has not been fully explored. This presents an area of opportunity, since COFs have demonstrated effectiveness in capturing this gas. Computational studies have been useful, as the predictions help select the material based on surface area, pore size, and, most importantly, the functional groups that could interact with the host molecule, saving time and energy in experiments and making the process more effective. Normally, H_2S is generated in a mixture with other interfering gases, and selectivity plays a key role in the manufacture of electronic devices for effective detection. COFs have demonstrated high selectivity in

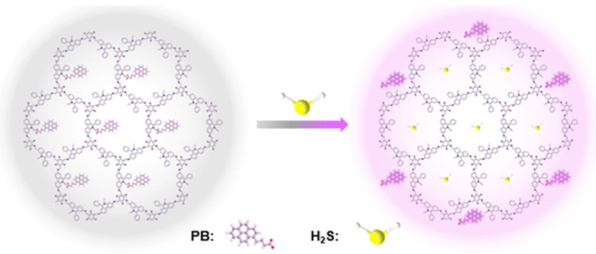

Fig. 11 (a) Synthesis of TpASH and its sequential post-synthesis modification. (b) Two-photon confocal fluorescence images of TpASH-NPHS in liver tissues of the cirrhotic mouse model at different CCl_4-treated periods. Scale bar: 300 μm. Adapted from ref. 76 with permission from Royal Society of Chemistry, copyright 2018.

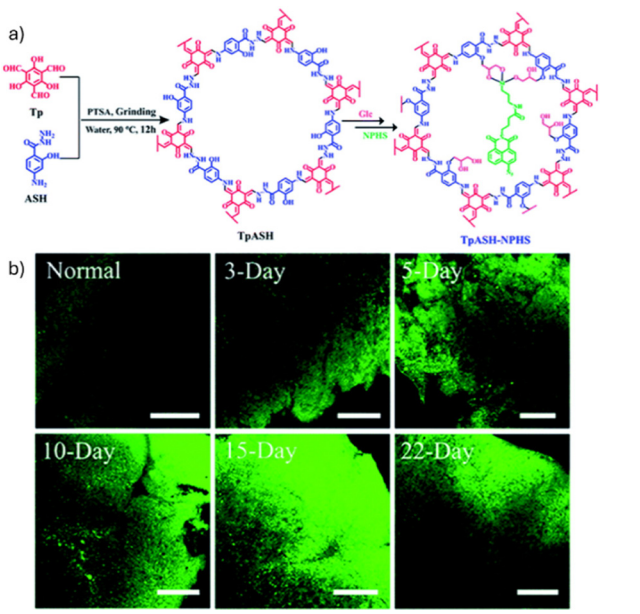

Fig. 12 Proposed mechanism of the EB-TFP@PB composite material sensor based on the IDA strategy. Adapted from ref. 78 with permission from Royal Society of Chemistry, copyright 2025.

several media, making them excellent candidates for this application. However, more studies are needed to advance their use in industrial processes.

Porous–organic cages and other materials

Porous–Organic Cages (POCs) are a distinct class of porous materials derived from the 3D covalent linkage of smaller organic molecules. The controlled supramolecular assembly of these molecular building blocks yields discrete, cage-like structures that exhibit diverse shapes and sizes. These structures possess access channels and internal cavities that permit the entry and trapping of external molecules compatible with the dimensions of the cavities. These materials exhibit high crystallinity, owing to their discrete molecular arrangement, and offer favorable processability as they are readily soluble in organic solvents. POCs also present flexible structures, which is an advantage over materials with rigid structures. This combination of properties provides the versatility needed for their incorporation into complex devices or for fulfilling specific applications, including gas capture and detection.[30,31,79]

Gas molecules are effectively trapped within the cavities of these cages by physical adsorption in the pores. When this dynamic trapping mechanism is coupled with the large surface area inherent to POCs, it results in significant gas capture, enhancing both the quantity and sensitivity of gas uptake. Since the chemistry and pore size of these materials are highly tunable, POCs can be specifically designed to optimize required functions. This optimization includes selectivity, load capacity, retention times, and the interaction strength between the host material and the gas molecule.[80] The potential of these materials for highly refined gas capture has generated significant interest in studying POCs for applications such as the separation and confinement of toxic gases, the removal of contaminants in waste management and the quantifiable detection of target molecules. A wide repertoire of such applications can be found in the literature, with several significant success stories published in recent years. These contributions encompass both the synthetic routes for obtaining POCs and the initial foundational studies on the capture and detection of toxic gases using these porous discrete materials.

Yuan and collaborators presented the synthesis of Imidazole-linked POCs (IPOCs), *via* the 1 : 4 reaction of a calix[4]resorcinarene derivative (C4RACHO) with monomers derived from 1,2-diaminobenzene units.[30] The materials proved to be prominent NH_3 adsorbents, achieving a remarkable capture capacity of 11.5 mmol g^{-1} at 1.0 bar and 25 °C. This exceptional performance is attributed to several factors: a large surface area (up to 1162 m^2 g^{-1}), high stability under extreme conditions, and the abundance of nitrogen-containing species within the pores that can form strong hydrogen bonds with ammonia molecules. Additionally, the sensing of dissolved ammonia was explored by leveraging the inherent luminescence of the material. A quenching effect was investigated using a prominent emission peak centered at 336 nm. This phenomenon involves a measurable decrease in the emission intensity after the material is exposed to the gas, demonstrating a high level of sensitivity capable of detecting a concentration change of just 10 μM of NH_3 in solution.

The material referred to as BTPOC, reported by Jiang *et al.*, effectively illustrates molecular recognition, exhibiting distinct adsorption behavior depending on the gas in contact.[79] Under identical conditions (0 °C and 1.0 bar), this material demonstrates high selectivity for CO_2 over both CH_4 and N_2. The substantial difference in gas uptake is evident; the CO_2 capture volume (42 cm^3 g^{-1}) is nearly four times greater than that of CH_4 (11.6 cm^3 g^{-1}) and approximately 40 times greater than that of N_2 (1.1 cm^3 g^{-1}). This superior selectivity is attributed to the enhanced affinity of CO_2 for the functional units present within the POC structure. When the bitiophene-based cyclohexanediamine and tetraaldehyde (BTDDP) blocks are assembled *via* aldehyde-amine condensation, specific preferential adsorption sites are created in the BTPOC. According to GCMC simulations performed at 25 °C and 1.0 bar, CO_2 molecules can extrinsically adsorb at these sites and subsequently diffuse through the interconnected pores. Similarly, sites rich in N and S promote the adsorption of other vapors, such as I_2.[81] BTPOC demonstrates the ability to reversibly capture up to 3.21 g g^{-1} of I_2.

Another case study for I_2 capture involves the porous organic cage designated PTC-2H, presented by Liu and collaborators in 2025.[31] The study demonstrated that the -NH bonds present in its porphyrin units serve as preferential sites for strong gas binding to the material. This POC is synthesized by the reaction of a porphyrin (PDBD) with cyclohexanediamine (CA). After purification and recrystallization, the resulting product exhibits a total surface area of 115 m^2 g^{-1} and shows a greater affinity for CO_2 over CH_4 and N_2. However, the most noteworthy feature is the progressive color change (from purple to black) of PTC-2H observed during the reaction. Adsorption reached a maximum capacity of 5.46 g g^{-1} for I_2 within the first 12 hours. This robust capture is attributed to chemisorption, resulting in exceptionally long retention times for I_2; more than 75% of the captured amount remains within the structure after 5 days. Furthermore, the material successfully demonstrated cyclic use, in which porphyrin rings and C=N bonds perform as effective adsorption sites. Collectively, these recent studies demonstrate the most contemporary advancements in the use of POCs as high-performance adsorbents for the capture and detection of toxic gases. All these materials offer acceptable capture capabilities and are specifically engineered for species that pose a significant health risk. To further enrich these substantial results, the study of POCs is being expanded to include other toxic gas species of interest. The capture and detection of H_2S using POCs for adsorption has also been proposed and successfully developed. This ongoing contribution is recognized for amplifying the range of toxic gases where POCs have demonstrated outstanding performance.

Capture of H_2S in POCs and other materials

Initial approaches specifically targeting the interaction of H_2S with POCs conventionally began with computational modeling

and calculations of the most extensively studied cage type: the cycloimine cage (CC). Specifically, the *in silico* work was proposed to accurately predict the adsorption capacity and the root-mean square deviation (RMSD) of the CC3 cage (Fig. 13a) towards various polluting gases, including H_2S.[82] By implementing GCMC simulations using the vdW3 force field coupled with the double-hybrid functional and scattering correction (B2PLYP-D3), it was possible to provide high reliability to the adsorbate–adsorbent interactions predicted by the calculations. This approach yielded a predicted H_2S gas capture of ≈2.4 mmol g^{-1} at 1.0 bar and 2 °C, suggesting that the flexibility of CC3 significantly influences the adsorption dynamics (Fig. 13b). The accuracy of the calculated force field (FF) depends on the *ab initio* method and the fitting procedure model, which is particularly crucial for modeling non-covalent interactions.[83] Since a purely intermolecular potential was considered for distant species, the simulations achieved a low RMSD value of 0.47 for CC3-H_2S and 0.23 for H_2S–H_2S interactions, respectively.

In 2024, another important computational study was presented, involving the interaction of H_2S with a different POC, designated CC1.[84] Similar in structure to CC3, CC1 features four triangular windows arranged in a tetrahedral geometry. In this model, DFT calculations with the B3LYP/6-311G(d, p) basis set were used to characterize interactions among various hazardous analytes, most notably H_2S. When trapped within the optimized CC1 cavity, the calculated interaction energy was −7.81 kcal mol^{-1}, which is characteristic of very weak physical adsorption of the dipolar H_2S molecule onto the cage, primarily mediated by hydrogen bonds and van der Waals forces. Charge decomposition analysis (CDA) was conducted to determine the relation between the donor–acceptor molecules present in the system. The analysis presented prominent binding sites exist where the nitrogen atoms of the cage could facilitate charge transfer to the gas molecule. This mechanism is predicted to result in extremely short recovery times (5.31×10^{-07} s) for H_2S release, suggesting excellent potential for the CC1 cage as a highly reusable adsorbent for this host molecule.

Building upon the computational background, the first experimental study focused on H_2S adsorption using these porous cages took place in 2025.[85] The surprising result of this work was that the ternary amine POC designated 6FT-RCC3 (Fig. 14a) achieved a record-breaking maximum H_2S capture capacity for a porous material (20.6 mmol g^{-1}) at room temperature and atmospheric pressure (Fig. 14b). Furthermore, it was experimentally confirmed that reversible adsorption is possible. Solid-state Nuclear Magnetic Resonance (RMN) and *in situ* DRIFT analysis confirmed the formation of hydrogen bonds between the gas and the nitrogen atoms of the cage, which act as anchoring sites. This leads to good cyclic regeneration and maintains a constant capture capacity, as previously predicted by computational models. The capture capacity of 6FT-RCC3 is even more remarkable considering that its surface area (339 m^2 g^{-1}) is not as large as other reported POCs. This is justified by the weak interactions between the H_2S–H_2S molecules themselves, facilitating their packing to achieve such high capture levels, as is the case with other polar host species.[86] To ornament this research, the limit of detection for H_2S was calculated, reaching 0.13 mM (≈4.43 ppm) for the analyte. This was achieved using the change in the material's fluorescence emission spectrum as a selective sensing technique upon saturation with H_2S. Employing sophisticated theoretical models offers significant advantages, as they facilitate the determination of the nature of the bond between the analyte and the cage, explain the specific binding sites where adsorption occurs, and justify the experimentally observed cyclic behavior. Finally, the proposed selectivity of these molecular fragments for H_2S over other gases was confirmed, with experimental results demonstrating a preferential binding and unique response that was not observed with CO_2, NO_2, SO_2, or water (Fig. 14c). This work presented the opportunity for these materials in applications in the capture and detection of toxic gases, such as H_2S.

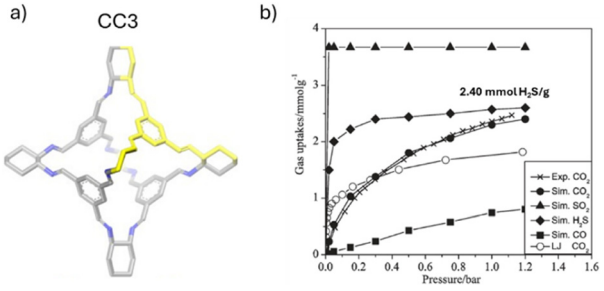

Fig. 13 (a) Molecular structure for CC3. (b) Adsorption curves of H_2S and other gases by CC3. Adapted from ref. 82 with permission from John Wiley and Sons, copyright 2014.

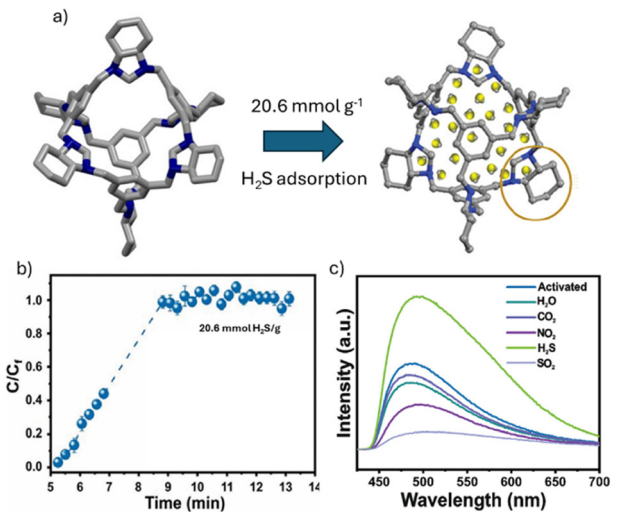

Fig. 14 (a) Modeling of optimized 6FT-RCC3 before and after H_2S saturation. (b) Breakthrough curves of H_2S adsorption by 6FT-RCC3 obtained at 25 °C and 1 bar. (c) Solid-state emission spectra of 6FT-RCC3 exposed to different gases under an excitation wavelength of 400 nm. Adapted from ref. 85 with permission from John Wiley and Sons, copyright 2025.

A clear order of magnitude difference is revealed when comparing the experimental results with the gas capture values predicted by computational calculations, including both GCMC and DFT models. This discrepancy is likely attributed to the dimensional limitations of computational modeling, as simulating the entire porous material is often difficult. Therefore, only simplified fractions of the POC are typically studied alongside the guest gas molecules.[84] This difference is further justified by the high degree of possible packing between the H_2S gas molecules themselves, a phenomenon that significantly favors increasing the final capture capacity and is often underestimated in simplified computational cells.

To enrich the discussion, the performance of POCs can be effective compared to that of other discrete porous material alternatives for H_2S capture. In recent years, studies have focused on the capture of H_2S molecules using adsorbents such as Metal–Organic Cages (MOCs) and carbon nanospheres. The primary goals of this research have been to elucidate the nature of the interactions governing adsorption and to explore their potential for real-world applications.

Jiang *et al.* presented a metal-free H_2S adsorbent mesoporous carbon nanospheres decorated with pyridine and pyrrolic nitrogen (ranging from 2.0–4.5 wt%), designated N-OMCS-700.[87] This material demonstrated a substantial capture capacity of 13.4 mmol g^{-1} (0 °C, 1.0 bar) and achieved complete H_2S conversion at temperatures of 180 °C or higher. Critically, these nanospheres proved capable of being used cyclically up to five times while maintaining the original capture capacity. Thus, they presented dual-purpose porous materials intended for application in solving diverse gas adsorption problems. The abundance of pores and the surface chemistry, where nitrogen atoms favor the adsorption of H_2S.[88] The carbonization temperature of 700 °C was reported to improve crystallinity and surface area (1575 m^2 g^{-1}), thereby enabling rapid diffusion of molecules within the internal pores to reach the nitrogen-containing sites. Additionally, the selectivity of H_2S adsorption over other gases such as N_2, CH_4, and CO_2 was successfully predicted across a range of temperatures using DFT calculations and the Ideal Adsorption Solution Theory (IAST). This selectivity effect was attributed to the strong interaction between H_2S and the functionalized nitrogen sites, as well as to the optimal pore size (3.7 nm), favoring the specific entry of H_2S molecules into the cavities.

Detection of H_2S in POCs and other materials

For the detection of abnormal H_2S levels in biological systems, that are closely related to the expression of certain types of cancer, metal–organic cages (MOCs) with adaptable pore diameters have been utilized to selectively exclude other chemical species.[26] The essential characteristic of MOCs is their structure, which relies on metal–organic ligand coordination bonds to form discrete cages. The specific cage designated MOC-HSN1 is composed of palladium ions bonded to the ligand *N*,*N*′-bis(2-pyrazincarboxamide)-1,4-butane (BPAP). This cage was specifically employed to encapsulate a traditional H_2S detector (HSN1), which emits a fluorescent response at 530 nm. The primary objective was to employ a size exclusion strategy to prevent the activation of HSN1 by nitroreductase (NTR), an interfering molecule that also generates the target fluorescent response,[39] thereby avoiding false positives. The results demonstrated that the well-defined cavities and uniform pore sizes of the MOC allowed access exclusively to H_2S molecules, as they are approximately seven times smaller than NTR molecules (Fig. 15). This design enabled effective shielding based on molecular weight differences for the

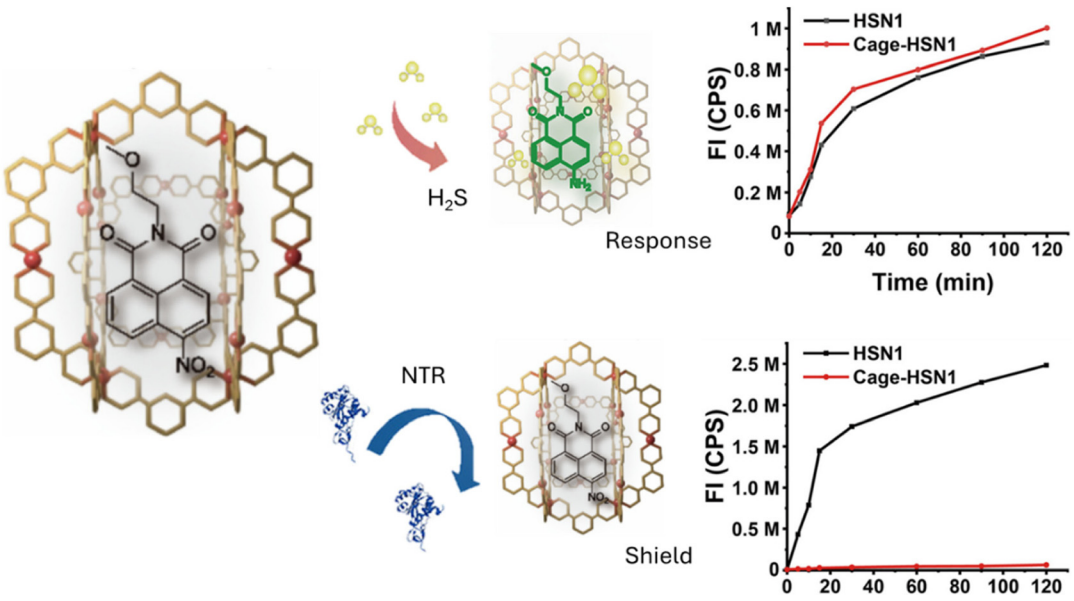

Fig. 15 Representation of the anti-interference shielding of the MOC-HSN1 system and the resulting fluorescence spectra. Adapted from ref. 26 with permission from Elsevier, copyright 2025.

Table 1 H_2S capture and detection of different porous cage-like materials

Material	System	H_2S capture	H_2S detection limit	Ref.
MOF Ni-CPO-27	Gas phase	12 mmol g^{-1}	—	33 and 37
MOF Mg-CUK-1	Gas phase	3.1 mmol g^{-1}	—	27
MOF Zr-fum	Gas phase	4.0 mmol g^{-1}	—	48
MOF Zr-mes		3.3 mmol g^{-1}		
MOF Zr-ita		1.3 mmol g^{-1}		
MOF MIL-53(Al)-TDC	Gas phase	18.6 mmol g^{-1}	—	49
MOF Mn-CUK-1	Gas phase	13.6 mmol g^{-1}	—	28
MOF MFM-300 (Sc)	Gas phase	10.2 mmol g^{-1}	—	34
MOF MFM-300 (In)		9.1 mmol g^{-1}		
SU-101		15.95 mmol g^{-1}		
$Zn_3(BTC)_2{\cdot}12H_2O$	Gas phase	—	4.4 ppm	35
ZIF-8			3 ppm	
Fum-fcu-MOF	Gas phase	—	5.4 ppb	51
IRMOF-3	Gas phase	—	28.3 μM	23
UiO-66-CH═CH_2	HEPES buffer	—	6.46 μM	52
MOF-5/CS/IL	Gas phase	—	1 ppm	53
SU-101	Gas phase and THF/H_2S solution	—	22 ppm	54
COF CTF-1-400–600	Gas phase	12.8 mmol g^{-1}	—	67
SiO_2@α-Fe_2O_3@COF	Gas phase	95.2%	—	68
COF-DC-8	Gas phase	—	204 ppb	38
CuCOF	H_2S in water	—	10 nM	74
COF TpASH-NPHS	Phosphate buffered solution	—	0.11 μM	76
COF EB-TFP	Gas phase	—	0.04 ppb	78
POC 6FT-RCC3	Gas phase and THF/H_2S solution	20.6 mmol g^{-1}	4.43 ppm	85
N-OMCS-700	Gas phase	13.4 mmol g^{-1}	—	87

analyte of interest, demonstrating that MOC-HSN1 functions as a molecular sensor that successfully eliminates NTR interference during H_2S quantification. The presentation of discrete porous materials as promising adsorbents is based not merely on the total amount of gas the material can retain, but also on the fact that their internal cavities can be rationally adjusted for selective capture. The ability to precisely control pore diameter, active binding sites, and physicochemical characteristics that favor the exclusion of molecules other than the analyte of interest is the defining feature that makes discrete materials, particularly POCs, advantageous compared to other classes of conventional adsorbents. The attributes of achieving specific confinement to a particular chemical species and being highly processable, not only in solids but also at different interfaces, are what make these materials exceptionally suited for real-world systems requiring gas capture, detection, and conversion (Table 1).

The quantification and removal of contaminants or waste treatment represent significant scopes in industrial applications where these materials offer a compelling and immediate solution.

Conclusions

Effective capture and detection of H_2S will become crucial in the coming years; traditional methods (*e.g.* membranes, wet scrubbing, metal oxides, zeolites) possess disadvantages; such as poor response, excessive use of water or solvents, corrosion or irreversible chemisorption. Hence, there is a need for new technologies to emerge and solve this problem. Porous cage-like materials present properties that can lead to new lines of study in the field of gas remediation. MOFs have dominated this field over the past decades. Through recent advances, MOFs present an interesting solution with the chemical transformation of H_2S into polysulfides, which can be used in other applications, like energy storage, presenting an alternative in waste valorization. On the other hand, COFs exhibit great stability and selectivity, making them excellent candidates for H_2S detection. The addition of other species, such as metal or fluorescent molecules, can enable rapid detection mechanisms, and studies have focused on this application. Finally, POCs are initiating a new revolution in porous materials for capturing and detecting toxic gases. Computational studies have demonstrated the possibility of this application and experimental works are starting to develop the methodologies for H_2S capture. Detection using these materials is an area of opportunity and more studies should appear in the upcoming years. The use of porous cage-like materials for the capture and detection of H_2S can lead to important advances in industrial applications. Future work is needed to ensure that these materials can present a solution to this environmental problem.

Author contributions

All authors contributed in writing the original draft, reviewing and editing the manuscript.

Conflicts of interest

There are no conflicts to declare.

Data availability

All data is available in the main text and we asked for the permission for the figures.

Acknowledgements

P. M. R., thanks SECIHTI for the Ph.D. fellowship (1277642). A. H. M. thanks SECIHTI for the MSc fellowship (1336791). We would like to express our gratitude to the Metropolitan Autonomous University of Mexico for financial support in the equipment maintenance.

References

1 Y. H. Chan, S. S. M. Lock, M. K. Wong, C. L. Yiin, A. C. M. Loy, K. W. Cheah, S. Y. W. Chai, C. Li, B. S. How, B. L. F. Chin, Z. P. Chan and S. S. Lam, A state-of-the-art review on capture and separation of hazardous hydrogen sulfide (H_2S): Recent advances, challenges and outlook, *Environ. Pollut.*, 2022, **314**, 120219, DOI: **10.1016/j.envpol.2022.120219**.

2 K. Kourtidis, A. Kelesis and M. Petrakakis, Hydrogen sulfide (H_2S) in urban ambient air, *Atmos. Environ.*, 2008, **42**, 7476–7482, DOI: **10.1016/j.atmosenv.2008.05.066**.

3 Z. Zhang, S. Jin, X. Teng, X. Duan, Y. Chen and Y. Wu, Hydrogen sulfide attenuates cardiac injury in takotsubo cardiomyopathy by alleviating oxidative stress, *Nitric Oxide*, 2017, **67**, 10–25, DOI: **10.1016/j.niox.2017.04.010**.

4 S. L. Malone Rubright, L. L. Pearce and J. Peterson, Environmental toxicology of hydrogen sulfide, *Nitric Oxide*, 2017, **71**, 1–13, DOI: **10.1016/j.niox.2017.09.011**.

5 D. A. Rahim, W. Fang, H. Wibowo, D. Hantoko, H. Susanto, K. Yoshikawa, Y. Zhong and M. Yan, Review of high temperature H_2S removal from syngas: Perspectives on downstream process integration, *Chem. Eng. Process. Process Intensif.*, 2023, **183**, 109258, DOI: **10.1016/j.cep.2022.109258**.

6 D. Mao, J. M. Griffin, R. Dawson, A. Fairhurst, G. Gupta and N. Bimbo, Porous materials for low-temperature H_2S-removal in fuel cell applications, *Sep. Purif. Technol.*, 2021, **277**, 119426, DOI: **10.1016/j.seppur.2021.119426**.

7 H. Furukawa, K. E. Cordova, M. O'Keeffe and O. M. Yaghi, The chemistry and applications of metal-organic frameworks, *Science*, 2013, **341**, 1230444, DOI: **10.1126/science.1230444**.

8 H. C. Zhou, J. R. Long and O. M. Yaghi, Introduction to metal-organic frameworks, *Chem. Rev.*, 2012, **112**, 673–674, DOI: **10.1021/cr300014x**.

9 A. I. B. Adrien, P. Côté, N. W. Ockwig, M. O'Keeffe, A. J. Matzger and O. M. Yaghi, Porous, Crystalline, Covalent Organic Frameworks, *Science*, 2005, **310**, 1166–1170, DOI: **10.1126/science.1120411**.

10 C. S. Diercks and O. M. Yaghi, The atom, the molecule, and the covalent organic framework, *Science*, 2017, **355**, eaal1585, DOI: **10.1126/science.aal1585**.

11 T. Tozawa, J. T. Jones, S. I. Swamy, S. Jiang, D. J. Adams, S. Shakespeare, R. Clowes, D. Bradshaw, T. Hasell, S. Y. Chong, C. Tang, S. Thompson, J. Parker, A. Trewin, J. Bacsa, A. M. Slawin, A. Steiner and A. I. Cooper, Porous organic cages, *Nat. Mater.*, 2009, **8**, 973–978, DOI: **10.1038/nmat2545**.

12 T. Hasell and A. I. Cooper, Porous organic cages: soluble, modular and molecular pores, *Nat. Rev. Mater.*, 2016, **1**, 16053, DOI: **10.1038/natrevmats.2016.53**.

13 X. Yang, Z. Ullah, J. F. Stoddart and C. T. Yavuz, Porous Organic Cages, *Chem. Rev.*, 2023, **123**, 4602–4634, DOI: **10.1021/acs.chemrev.2c00667**.

14 T. R. Cook and P. J. Stang, Recent Developments in the Preparation and Chemistry of Metallacycles and Metallacages via Coordination, *Chem. Rev.*, 2015, **115**, 7001–7045, DOI: **10.1021/cr5005666**.

15 J. Mi, F. Liu, W. Chen, X. Chen, L. Shen, Y. Cao, C. Au, K. Huang, A. Zheng and L. Jiang, Design of Efficient, Hierarchical Porous Polymers Endowed with Tunable Structural Base Sites for Direct Catalytic Elimination of COS and H_2S, *ACS Appl. Mater. Interfaces*, 2019, **11**, 29950–29959, DOI: **10.1021/acsami.9b09149**.

16 J. S. Eow, Recovery of sulfur from sour acid gas: A review of the technology, *Environ. Prog.*, 2004, **21**, 143–162, DOI: **10.1002/ep.670210312**.

17 F. Tari, M. Shekarriz, S. Zarrinpashne and A. Ruzbehani, Design and implementation of an effective system for catalytic degassing of claus-derived molten sulfur over monometallic and bimetallic nanosilica-based catalysts and optimization via RSM-CCD, *J. Nat. Gas Sci. Eng.*, 2018, **59**, 124–135, DOI: **10.1016/j.jngse.2018.08.004**.

18 T. Yu, Z. Chen, Z. Liu, J. Xu and Y. Wang, Review of Hydrogen Sulfide Removal from Various Industrial Gases by Zeolites, *Separations*, 2022, **9**, 229, DOI: **10.3390/separations9090229**.

19 M. S. Aminuddin, M. A. Bustam and K. Johari, Latest technological advances and insights into capture and removal of hydrogen sulfide: a critical review, *RSC Sustain.*, 2024, **2**, 757–803, DOI: **10.1039/d3su00484h**.

20 A. Pudi, M. Rezaei, V. Signorini, M. P. Andersson, M. G. Baschetti and S. S. Mansouri, Hydrogen sulfide capture and removal technologies: A comprehensive review of recent developments and emerging trends, *Sep. Purif. Technol.*, 2022, **298**, 121448, DOI: **10.1016/j.seppur.2022.121448**.

21 J. L. Obeso, D. R. Amaro, C. V. Flores, A. Gutiérrez-Alejandre, R. A. Peralta, C. Leyva and I. A. Ibarra, Chemical transformations of highly toxic H_2S to promising clean energy in MOFs, *Coord. Chem. Rev.*, 2023, **485**, 215135, DOI: **10.1016/j.ccr.2023.215135**.

22 V. Pandey and T. Pandey, Hydrogen sulfide detection: Recent advancement and future perspectives towards fluorescence as a versatile Biophysical method, *Nitric Oxide*, 2025, **157**, 34–45, DOI: **10.1016/j.niox.2025.04.004**.

23 X. Zhang, J. Zhang, Q. Hu, Y. Cui, Y. Yang and G. Qian, Postsynthetic modification of metal–organic framework for

hydrogen sulfide detection, *Appl. Surf. Sci.*, 2015, **355**, 814–819, DOI: 10.1016/j.apsusc.2015.07.166.

24 K. Vikrant, V. Kumar, Y. S. Ok, K.-H. Kim and A. Deep, Metal-organic framework (MOF)-based advanced sensing platforms for the detection of hydrogen sulfide, *Trends Anal. Chem.*, 2018, **105**, 263–281, DOI: 10.1016/j.trac.2018.05.013.

25 P. M. May, D. Batka, G. Hefter, E. Konigsberger and D. Rowland, Goodbye to S^{2-} in aqueous solution, *Chem. Commun.*, 2018, **54**, 1980–1983, DOI: 10.1039/c8cc00187a.

26 X. Tan, Y. Huang, Y. Luo, Z. Lin, X. Shi, Z. Zeng, J. Chen and C. Zhao, A molecular-size sieve-inspired metal-organic cage-based hydrogen sulfide probe for colon cancer diagnosis, *Chem. Eng. J.*, 2025, **519**, 164859, DOI: 10.1016/j.cej.2025.164859.

27 E. Sánchez-González, P. G. M. Mileo, M. Sagastuy-Breña, J. R. Álvarez, J. E. Reynolds, A. Villarreal, A. Gutiérrez-Alejandre, J. Ramírez, J. Balmaseda, E. González-Zamora, G. Maurin, S. M. Humphrey and I. A. Ibarra, Highly reversible sorption of H_2S and CO_2 by an environmentally friendly Mg-based MOF, *J. Mater. Chem. A*, 2018, **6**, 16900–16909, DOI: 10.1039/c8ta05400b.

28 S. G. Dunning, N. K. Gupta, J. E. Reynolds 3rd, M. Sagastuy-Brena, J. G. Flores, E. Martinez-Ahumada, E. Sanchez-Gonzalez, V. M. Lynch, A. Gutierrez-Alejandre, J. Aguilar-Pliego, K. S. Kim, I. A. Ibarra and S. M. Humphrey, Mn-CUK-1: A Flexible MOF for SO_2, H_2O, and H_2S Capture, *Inorg. Chem.*, 2022, **61**, 15037–15044, DOI: 10.1021/acs.inorgchem.2c02012.

29 X. Zhao, L. Zhang, J. Bai, P. Wu, Y. Li, L. Liang, L. Xie and J. Wang, A copper-based metal-organic framework for ratiometric detection of hydrogen sulfide with high sensitivity and fast response, *Spectrochim. Acta, Part A*, 2020, **243**, 118794, DOI: 10.1016/j.saa.2020.118794.

30 G. Zhang, N. Xu, M. Yang, W. Wang, K. Su and D. Yuan, Ultrastable Imidazole-linked Porous Organic Cages for Ammonia Capture and Detection, *Angew. Chem., Int. Ed.*, 2025, **64**, e202423226, DOI: 10.1002/anie.202423226.

31 Z. Wang, J. Li, Z. Du, L. Pang and C. Liu, Metal-free porphyrin porous organic cage for efficient iodine capture, *Chem. Eng. J.*, 2025, **509**, 161326, DOI: 10.1016/j.cej.2025.161326.

32 T. L. G. Hoang, D. T. Doan, S. Nanda, R. Lavoie and P. Nguyen-Tri, Development of metal-organic framework-based systems for H_2S removal: A comprehensive review, *Coord. Chem. Rev.*, 2025, **529**, 216466, DOI: 10.1016/j.ccr.2025.216466.

33 P. K. Allan, P. S. Wheatley, D. Aldous, M. I. Mohideen, C. Tang, J. A. Hriljac, I. L. Megson, K. W. Chapman, G. De Weireld, S. Vaesen and R. E. Morris, Metal-organic frameworks for the storage and delivery of biologically active hydrogen sulfide, *Dalton Trans.*, 2012, **41**, 4060–4066, DOI: 10.1039/c2dt12069k.

34 A. López-Olvera, J. G. Flores, J. Aguilar-Pliego, C. K. Brozek, A. Gutiérrez-Alejandre and I. A. Ibarra, Chemical Transformation of H_2S within the Pores of Metal–Organic Frameworks: Formation of Polysulfides, *Chem. Mater.*, 2021, **33**, 6269–6276, DOI: 10.1021/acs.chemmater.1c01918.

35 X. Wan, L. Wu, L. Zhang, H. Song and Y. Lv, Novel metal-organic frameworks-based hydrogen sulfide cataluminescence sensors, *Sens. Actuators, B*, 2015, **220**, 614–621, DOI: 10.1016/j.snb.2015.05.125.

36 H. Feng, S. Guo, Y. Guo, Q. Zhao, Y. Xia, Z. Duan, M. Hou, L. Yang, L. Gao and H. Tai, Advances in metal-organic framework-based hydrogen sulfide gas sensors, *Coord. Chem. Rev.*, 2026, **546**, 217087, DOI: 10.1016/j.ccr.2025.217087.

37 S. Chavan, F. Bonino, L. Valenzano, B. Civalleri, C. Lamberti, N. Acerbi, J. H. Cavka, M. Leistner and S. Bordiga, Fundamental Aspects of H_2S Adsorption on CPO-27-Ni, *J. Phys. Chem. C*, 2013, **117**, 15615–15622, DOI: 10.1021/jp402440u.

38 Z. Meng, R. M. Stolz and K. A. Mirica, Two-Dimensional Chemiresistive Covalent Organic Framework with High Intrinsic Conductivity, *J. Am. Chem. Soc.*, 2019, **141**, 11929–11937, DOI: 10.1021/jacs.9b03441.

39 L. J. O'Connor, I. N. Mistry, S. L. Collins, L. K. Folkes, G. Brown, S. J. Conway and E. M. Hammond, CYP450 Enzymes Effect Oxygen-Dependent Reduction of Azide-Based Fluorogenic Dyes, *ACS Cent. Sci.*, 2017, **3**, 20–30, DOI: 10.1021/acscentsci.6b00276.

40 V. F. Yusuf, N. I. Malek and S. K. Kailasa, Review on Metal-Organic Framework Classification, Synthetic Approaches, and Influencing Factors: Applications in Energy, Drug Delivery, and Wastewater Treatment, *ACS Omega*, 2022, **7**, 44507–44531, DOI: 10.1021/acsomega.2c05310.

41 K. K. Gangu, S. Maddila, S. B. Mukkamala and S. B. Jonnalagadda, A review on contemporary Metal–Organic Framework materials, *Inorg. Chim. Acta*, 2016, **446**, 61–74, DOI: 10.1016/j.ica.2016.02.062.

42 X. L. Zhao, J. L. Liu, F. T. Xie, T. Yang, R. Hu and Y. H. Yang, Iodide-enhanced Co/Fe-MOFs nanozyme for sensitively colorimetric detection of H_2S, *Spectrochim. Acta, Part A*, 2021, **262**, 120117, DOI: 10.1016/j.saa.2021.120117.

43 J. Zhou, X. Gao, X. Chen, H. Sun, X. Li, L. Shi and Y. Liu, Bi-MOF-based point-of-care testing paper for dual-mode detection of H_2S, *Biosens. Bioelectron.*, 2025, **270**, 116934, DOI: 10.1016/j.bios.2024.116934.

44 R. Song, L. Hou, Y. Wang, Y. Li, X. Wang, Y. Zang, Y. Zang, X. Wang and S. Yan, Fluorescence Zn-based metal–organic frameworks for the detection of hydrogen sulfide in natural gas, *Anal. Methods*, 2017, **9**, 3914–3919, DOI: 10.1039/c7ay01193h.

45 X. Zheng, R. Fan, Y. Song, A. Wang, K. Xing, X. Du, P. Wang and Y. Yang, A highly sensitive turn-on ratiometric luminescent probe based on postsynthetic modification of Tb^{3+}@Cu-MOF for H_2S detection, *J. Mater. Chem. C*, 2017, **5**, 9943–9951, DOI: 10.1039/c7tc02430d.

46 K. Yu, M. Li, H. Chai, Q. Liu, X. Hai, M. Tian, L. Qu, T. Xu, G. Zhang and X. Zhang, MOF-818 nanozyme-based colorimetric and electrochemical dual-mode smartphone

sensing platform for in situ detection of H_2O_2 and H_2S released from living cells, *Chem. Eng. J.*, 2023, **451**, 138321, DOI: 10.1016/j.cej.2022.138321.

47 T. Ma, X. Liu, X. Wang, J. G. Ma and P. Cheng, Bottom-Up Construction of Rhombic Lamellar CoNi-MOFs for the Electrochemical Sensing of H(2)S, *Inorg. Chem.*, 2024, **63**, 7504–7511, DOI: 10.1021/acs.inorgchem.4c00862.

48 F. E. Chen, R. M. Mandel, J. J. Woods, J. H. Lee, J. Kim, J. H. Hsu, J. J. Fuentes-Rivera, J. J. Wilson and P. J. Milner, Biocompatible metal-organic frameworks for the storage and therapeutic delivery of hydrogen sulfide, *Chem. Sci.*, 2021, **12**, 7848–7857, DOI: 10.1039/d1sc00691f.

49 J. A. Zarate, E. Sanchez-Gonzalez, T. Jurado-Vazquez, A. Gutierrez-Alejandre, E. Gonzalez-Zamora, I. Castillo, G. Maurin and I. A. Ibarra, Outstanding reversible H_2S capture by an Al(iii)-based MOF, *Chem. Commun.*, 2019, **55**, 3049–3052, DOI: 10.1039/c8cc09379b.

50 R. A. Marquez, J. L. Obeso, R. R. Vaidyula, V. B. López-Cervantes, R. A. Peralta, P. Marín Rosas, J. A. de los Reyes, C. B. Mullins and I. A. Ibarra, From pollution to energy storage: leveraging hydrogen sulfide with SU-101 cathodes in lithium–sulfur batteries, *J. Mater. Chem. A*, 2024, **12**, 32735–32744, DOI: 10.1039/d4ta03620d.

51 O. Yassine, O. Shekhah, A. H. Assen, Y. Belmabkhout, K. N. Salama and M. Eddaoudi, H_2S Sensors: Fumarate-Based fcu-MOF Thin Film Grown on a Capacitive Interdigitated Electrode, *Angew. Chem., Int. Ed.*, 2016, **55**, 15879–15883, DOI: 10.1002/anie.201608780.

52 Y. Li, X. Zhang, L. Zhang, K. Jiang, Y. Cui, Y. Yang and G. Qian, A nanoscale Zr-based fluorescent metal-organic framework for selective and sensitive detection of hydrogen sulfide, *J. Solid State Chem.*, 2017, **255**, 97–101, DOI: 10.1016/j.jssc.2017.07.027.

53 A. Ali, A. Alzamly, Y. E. Greish, M. Bakiro, H. L. Nguyen and S. T. Mahmoud, A Highly Sensitive and Flexible Metal-Organic Framework Polymer-Based H_2S Gas Sensor, *ACS Omega*, 2021, **6**, 17690–17697, DOI: 10.1021/acsomega.1c02295.

54 V. B. Lopez-Cervantes, J. L. Obeso, J. G. Flores, A. Gutierrez-Alejandre, R. A. Marquez, J. A. de Los Reyes, C. V. Flores, N. S. Portillo-Velez, P. Marin-Rosas, C. A. Celaya, E. Gonzalez-Zamora, D. Solis-Ibarra, R. A. Peralta and I. A. Ibarra, Formation of polysulfides as a smart strategy to selectively detect H_2S in a Bi(iii)-based MOF material, *Chem. Sci.*, 2025, **16**, 5483–5492, DOI: 10.1039/d4sc07144a.

55 Y. Huang, X. Hao, S. Ma, R. Wang and Y. Wang, Covalent organic framework-based porous materials for harmful gas purification, *Chemosphere*, 2022, **291**, 132795, DOI: 10.1016/j.chemosphere.2021.132795.

56 Q. Guan, L. L. Zhou and Y. B. Dong, Metalated covalent organic frameworks: from synthetic strategies to diverse applications, *Chem. Soc. Rev.*, 2022, **51**, 6307–6416, DOI: 10.1039/d1cs00983d.

57 Y. Song, Q. Sun, B. Aguila and S. Ma, Opportunities of Covalent Organic Frameworks for Advanced Applications, *Adv. Sci.*, 2019, **6**, 1801410, DOI: 10.1002/advs.201801410.

58 K. Geng, T. He, R. Liu, S. Dalapati, K. T. Tan, Z. Li, S. Tao, Y. Gong, Q. Jiang and D. Jiang, Covalent Organic Frameworks: Design, Synthesis, and Functions, *Chem. Rev.*, 2020, **120**, 8814–8933, DOI: 10.1021/acs.chemrev.9b00550.

59 A. Natraj, W. Ji, J. Xin, I. Castano, D. W. Burke, A. M. Evans, M. J. Strauss, M. Ateia, L. S. Hamachi, N. C. Gianneschi, A. L. Za, J. Sun, K. Yusuf and W. R. Dichtel, Single-Crystalline Imine-Linked Two-Dimensional Covalent Organic Frameworks Separate Benzene and Cyclohexane Efficiently, *J. Am. Chem. Soc.*, 2022, **144**, 19813–19824, DOI: 10.1021/jacs.2c07166.

60 H. Fan, J. Gu, H. Meng, A. Knebel and J. Caro, High-Flux Membranes Based on the Covalent Organic Framework COF-LZU1 for Selective Dye Separation by Nanofiltration, *Angew. Chem., Int. Ed.*, 2018, **57**, 4083–4087, DOI: 10.1002/anie.201712816.

61 X. Wang, L. Chen, S. Y. Chong, M. A. Little, Y. Wu, W. H. Zhu, R. Clowes, Y. Yan, M. A. Zwijnenburg, R. S. Sprick and A. I. Cooper, Sulfone-containing covalent organic frameworks for photocatalytic hydrogen evolution from water, *Nat. Chem.*, 2018, **10**, 1180–1189, DOI: 10.1038/s41557-018-0141-5.

62 L. Zhong, J. Liu, Y. Xiao, Z. Song, L. Chen, G. Li and Y. Wu, Advanced strategies of covalent organic framework nanomedicines in targeting and overcoming biological barriers, *Asian J. Pharm. Sci.*, 2025, **20**, 101066, DOI: 10.1016/j.ajps.2025.101066.

63 S. Ge, K. Wei, W. Peng, R. Huang, E. Akinlabi, H. Xia, M. W. Shahzad, X. Zhang, B. B. Xu and J. Jiang, A comprehensive review of covalent organic frameworks (COFs) and their derivatives in environmental pollution control, *Chem. Soc. Rev.*, 2024, **53**, 11259–11302, DOI: 10.1039/d4cs00521j.

64 F. Amjad, A. Umar, M. H. Saeed, M. S. Nazir, Z. Ali, K. A. Lin, J. Lee, S. U. Hassan, M. Hussain and Y. K. Park, Unlocking the Comparative Potential of Porous Frameworks: A Review on MOFs and COFs for Gas Sorption, *Top. Curr. Chem.*, 2025, **383**, 32, DOI: 10.1007/s41061-025-00517-9.

65 N. Huang, X. Chen, R. Krishna and D. Jiang, Two-dimensional covalent organic frameworks for carbon dioxide capture through channel-wall functionalization, *Angew. Chem., Int. Ed.*, 2015, **54**, 2986–2990, DOI: 10.1002/anie.201411262.

66 G. Y. Lee, J. Lee, H. T. Vo, S. Kim, H. Lee and T. Park, Amine-Functionalized Covalent Organic Framework for Efficient SO_2 Capture with High Reversibility, *Sci. Rep.*, 2017, **7**, 557, DOI: 10.1038/s41598-017-00738-z.

67 W. L. Peng, X. Kan, W. Chen, J. Mi, G. Zhang, Y. Xiao, W. Liu, F. Liu and A. Zheng, Efficiently Selective Oxidation of H_2S to Elemental Sulfur over Covalent Triazine Framework Catalysts, *ACS Appl. Mater. Interfaces*, 2021, **13**, 34124–34133, DOI: 10.1021/acsami.1c06667.

68 Y. Pan, Z. Huang, D. Zheng and C. Yang, Interface engineering of sandwich SiO_2@alpha-Fe_2O_3@COF core-shell S-scheme heterojunctions for efficient photocatalytic oxidation of gas-phase H_2S, *J. Colloid Interface Sci.*, 2023, **644**, 19–28, DOI: 10.1016/j.jcis.2023.03.195.

69 H. Wang, X. Zeng, W. Wang and D. Cao, Selective capture of trace sulfur gas by porous covalent-organic materials, *Chem. Eng. Sci.*, 2015, **135**, 373–380, DOI: **10.1016/j.ces.2015.02.015**.

70 G. O. Aksu, I. Erucar, Z. P. Haslak and S. Keskin, Exploring covalent organic frameworks for H_2S + CO_2 separation from natural gas using efficient computational approaches, *J. CO_2 Util.*, 2022, **62**, 102077, DOI: **10.1016/j.jcou.2022.102077**.

71 Z. Meng and K. A. Mirica, Covalent organic frameworks as multifunctional materials for chemical detection, *Chem. Soc. Rev.*, 2021, **50**, 13498–13558, DOI: **10.1039/d1cs00600b**.

72 L. X. Chengyue Yu, F. Zhao, L. Kong, Y. Chen, L. Li, Z. Zhu and L. Jiang, Multiscale Covalent Organic Framework (COF) Films for Task-Specific Sensing in Multicomponent Gases, *ACS Mater. Lett.*, 2024, **12**, 5454–5478, DOI: **10.1021/acsmaterialslett.4c01672**.

73 W. Zhao, J. L. Obeso, V. B. Lopez-Cervantes, M. Bahri, E. Sanchez-Gonzalez, Y. A. Amador-Sanchez, J. Ren, N. D. Browning, R. A. Peralta, G. Barcaro, S. Monti, D. Solis-Ibarra, I. A. Ibarra and D. Zhao, Achieving Sub-ppm Sensitivity in SO_2 Detection with a Chemically Stable Covalent Organic Framework, *Angew. Chem., Int. Ed.*, 2025, **64**, e202415088, DOI: **10.1002/anie.202415088**.

74 X. Ge, H. Zhang, C. Zhang and M. Du, A Heterogeneous Nanoscale Covalent Organic Framework Fluorescence Probe for Sensitive Detection of Hydrogen Sulfide, *ChemNanoMat*, 2021, **7**, 530–533, DOI: **10.1002/cnma.202100049**.

75 G. Lin, H. Ding, R. Chen, Z. Peng, B. Wang and C. Wang, 3D Porphyrin-Based Covalent Organic Frameworks, *J. Am. Chem. Soc.*, 2017, **139**, 8705–8709, DOI: **10.1021/jacs.7b04141**.

76 P. Wang, F. Zhou, C. Zhang, S. Y. Yin, L. Teng, L. Chen, X. X. Hu, H. W. Liu, X. Yin and X. B. Zhang, Ultrathin two-dimensional covalent organic framework nanoprobe for interference-resistant two-photon fluorescence bioimaging, *Chem. Sci.*, 2018, **9**, 8402–8408, DOI: **10.1039/c8sc03393e**.

77 J. Feng, W. X. Ren, F. Kong and Y. B. Dong, A covalent organic framework-based nanoagent for H_2S-activable phototherapy against colon cancer, *Chem. Commun.*, 2021, **57**, 7240–7243, DOI: **10.1039/d1cc02258j**.

78 C. Chu, X. Lian, Q. Zheng, Y. Tao, Y. Qin and J. Wang, Functional covalent organic framework H_2S sensors for periodontitis monitoring and antibacterial treatment, *New J. Chem.*, 2025, **49**, 4198–4204, DOI: **10.1039/d4nj05111d**.

79 C. Liu, W. Li, Y. Liu, H. Wang, B. Yu, Z. Bao and J. Jiang, Porous organic cages for efficient gas selective separation and iodine capture, *Chem. Eng. J.*, 2022, **428**, 131129, DOI: **10.1016/j.cej.2021.131129**.

80 M. L. Martinez, P. Marin-Rosas, V. B. Lopez-Cervantes, A. Guzman-Vargas, R. A. Peralta, D. Solis-Ibarra and I. A. Ibarra, Fluorescence spectroscopy: detection and sensing of SO_2 and H_2S using MOFs and other emerging porous materials, *Dalton Trans.*, 2025, **54**, 13806–13819, DOI: **10.1039/d5dt01521a**.

81 T. Hasell, M. Schmidtmann and A. I. Cooper, Molecular doping of porous organic cages, *J. Am. Chem. Soc.*, 2011, **133**, 14920–14923, DOI: **10.1021/ja205969q**.

82 W. Li and J. Zhang, Multiscale simulation of pollution gases adsorption in porous organic cage CC3, *J. Comput. Chem.*, 2013, **35**, 174–180, DOI: **10.1002/jcc.23486**.

83 S. Grimme, J. Antony, S. Ehrlich and H. Krieg, A consistent and accurate *ab initio* parametrization of density functional dispersion correction (DFT-D) for the 94 elements H-Pu, *J. Chem. Phys.*, 2010, **132**, 154104, DOI: **10.1063/1.3382344**.

84 S. Rani, R. Hussain, S. Aslam, S. Sarfaraz, A. Hussain, M. D. S. Haider, M. A. Yawer, M. Imran and K. Ayub, Peculiar trapping behavior of porous organic nanocage CC1 towards H_2S, SF_6, SF_4, $SOCl_2$ and SO_2; A DFT Perspective, *Comput. Theor. Chem.*, 2024, **1241**, 114898, DOI: **10.1016/j.comptc.2024.114898**.

85 J. L. Obeso, D. Hu, V. B. Lopez-Cervantes, Y. A. Amador-Sanchez, C. V. Flores, J. G. Flores, S. Ling, E. Lima, A. Gutierrez-Alejandre, M. A. Vera, R. A. Peralta, J. A. de Los Reyes, D. Solis-Ibarra, I. A. Ibarra and M. Liu, Record-Breaking H_2S Capture and ppm-Level Sensing with a Chemically Stable Porous Organic Cage, *Small*, 2025, **21**, e2408155, DOI: **10.1002/smll.202408155**.

86 E. Martinez-Ahumada, D. He, V. Berryman, A. Lopez-Olvera, M. Hernandez, V. Jancik, V. Martis, M. A. Vera, E. Lima, D. J. Parker, A. I. Cooper, I. A. Ibarra and M. Liu, SO_2 Capture Using Porous Organic Cages, *Angew. Chem., Int. Ed.*, 2021, **60**, 17556–17563, DOI: **10.1002/anie.202104555**.

87 X. Kan, X. Chen, W. Chen, J. Mi, J.-Y. Zhang, F. Liu, A. Zheng, K. Huang, L. Shen, C. Au and L. Jiang, Nitrogen-Decorated, Ordered Mesoporous Carbon Spheres as High-Efficient Catalysts for Selective Capture and Oxidation of H_2S, *ACS Sustainable Chem. Eng.*, 2019, **7**, 7609–7618, DOI: **10.1021/acssuschemeng.8b05852**.

88 M. Khabazipour and M. Anbia, Removal of Hydrogen Sulfide from Gas Streams Using Porous Materials: A Review, *Ind. Eng. Chem. Res.*, 2019, **58**, 22133–22164, DOI: **10.1021/acs.iecr.9b03800**.